Technical Report Documentation Page

1. Report No. FHWA/TX-08/0-4563-1	2. Government Accession No.	3. Recipient's Catalog No.
4. Title and Subtitle Prediction Model for Concrete Behavior—Final Report		5. Report Date October 2007, Rev. May 2008 6. Performing Organization Code
7. Author(s) Kevin J. Folliard, Maria Juenger, Anton Schindler, Kyle Riding, Jonathan Poole, Loukas F. Kallivokas, Samuel Slatnick, Jared Whigham, J.L. Meadows		8. Performing Organization Report No. 0-4563-1
9. Performing Organization Name and Address Center for Transportation Research The University of Texas at Austin 3208 Red River, Suite 200 Austin, TX 78705-2650		10. Work Unit No. (TRAIS) 11. Contract or Grant No. 0-4563
12. Sponsoring Agency Name and Address Texas Department of Transportation Research and Technology Implementation Office P.O. Box 5080 Austin, TX 78763-5080		13. Type of Report and Period Covered Technical Report September 2002- August 2007 14. Sponsoring Agency Code

15. Supplementary Notes
Project performed in cooperation with the Texas Department of Transportation and the Federal Highway Administration.

16. Abstract
This report summarizes work performed under Texas Department of Transportation (TxDOT) Project 4563, *Prediction Model for Concrete Behavior.* The main product developed under this project is a software program, named *Concrete Works*, which gives laboratory technicians, engineers, and contractors a tool that combines concrete design, analysis, and performance prediction to improve and optimize the performance of concrete structures.

A unique feature of the testing performed is the use of rigid cracking frames. This test was developed in Germany, and measures the cracking sensitivity of a restrained dog-bone-shaped concrete specimen from the time of concrete placement. Temperature-controlled formwork is used to cure the specimen to match field conditions of mass concrete members. These frames are designed to allow fresh concrete to be cast into their formwork, which enables the study of very early-age behavior of concrete mixtures. More than 70 tests have been completed to date and these results were used to characterize the very early-age creep behavior and risk of cracking of various concretes. Mixture-specific heat of hydration values are used to accurately model the effect of various cementitious materials material on the in-place concrete temperature distribution. The model has been calibrated with over 33,000 hours of temperature data collected from field sites. The software provides detailed results to check compliance with specification to control thermal cracking, alkali silica reaction, delayed ettringite formation, and service-life expectancy.

This report concludes with a section aimed at implementing ConcreteWorks, with emphasis on how best to use, specify, and check compliance with mass concrete design guidelines.

17. Key Words prediction model, concrete, concreteworks	18. Distribution Statement No restrictions. This document is available to the public through the National Technical Information Service, Springfield, Virginia 22161; www.ntis.gov.

19. Security Classif. (of report)	20. Security Classif. (of this page)	21. No. of pages	22. Price
Unclassified	Unclassified	78	

Form DOT F 1700.7 (8-72) Reproduction of completed page authorized

Prediction Model for Concrete Behavior—Final Report

Kevin J. Folliard
Maria Juenger
Anton Schindler
Kyle Riding
Jonathan Poole
Loukas F. Kallivokas
Samuel Slatnick
Jared Whigham
J.L. Meadows

CTR Technical Report:	0-4563-1
Report Date:	October 2007, Rev. May 2008
Research Project:	0-4563
Research Project Title:	Prediction Model for Concrete Behavior
Sponsoring Agency:	Texas Department of Transportation
Performing Agency:	Center for Transportation Research at The University of Texas at Austin

Project performed in cooperation with the Texas Department of Transportation and the Federal Highway Administration.

Center for Transportation Research
The University of Texas at Austin
3208 Red River
Austin, TX 78705

www.utexas.edu/research/ctr

Disclaimers

Authors' Disclaimer: The contents of this report reflect the views of the authors, who are responsible for the facts and the accuracy of the data presented herein. The contents do not necessarily reflect the official view or policies of the Federal Highway Administration or the Texas Department of Transportation. This report does not constitute a standard, specification, or regulation.

Patent Disclaimer: There was no invention or discovery conceived or first actually reduced to practice in the course of or under this contract, including any art, method, process, machine manufacture, design or composition of matter, or any new useful improvement thereof, or any variety of plant, which is or may be patentable under the patent laws of the United States of America or any foreign country.

Engineering Disclaimer

NOT INTENDED FOR CONSTRUCTION, BIDDING, OR PERMIT PURPOSES.

Project Engineer: David W. Fowler
Professional Engineer License Number: Texas No. 27859
P. E. Designation: Researcher

Acknowledgments

The authors express appreciation to the TxDOT Project Director (Ralph Browne), members of the Project Monitoring Committee, and the staff at the Concrete Durability Center.

Table of Contents

List of Figures

List of Tables

1. Introduction

The cost of repairing or replacing bridges that are not functionally obsolete is staggering. The premature deterioration of our infrastructure from cracking and concrete material related durability problems can be prevented. To ensure a long service life for a concrete structure it is critical to plan appropriately during the design phase and to take appropriate precautions during the construction phase. Consideration of the causes of concrete deterioration during construction planning can ensure a maximum use of locally available, cost effective materials, improve construction efficiency and speed, and ensure a durable structure.

In order for engineers and contractors to consider concrete durability in the design and construction planning stages, these professionals need to understand the issues affecting a structure's service life. They also need a simple, user-friendly method or tool that will allow them to quickly evaluate the effectiveness of alternative methods and materials. As part of this research, a user-friendly software package named ConcreteWorks has been developed that allows users to compare how different materials and construction techniques affect the structure's durability against several causes of premature deterioration.

This chapter gives an overview of some of the commonly occurring causes of premature concrete degradation. Chapter 2 presents the heat of hydration model developed and the research behind it. Chapter 3 details the temperature prediction model developed for ConcreteWorks and provides comparison with field site data. Chapter 4 explains the various early-age models that combine to estimate the in-place performance of a specific concrete member. Chapter 5 provides insight into the uses of the program. Chapter 6 describes how the project outcomes should be implemented, including proposed specification changes. Chapter 7 provides a summary, an explanation of economic benefits, and recommended further research.

Much more detail on the laboratory evaluations, field studies, and modeling efforts can be found in Ph.D. dissertations by Poole (2007) and Riding (2007), as well as MS theses by Whigham (2005) and Meadows (2007).

1.1 Thermal Cracking

1.1.1 Problem

A large amount of heat is released during the chemical reaction between cementitious materials and water. The heat released during this chemical reaction known as hydration will not easily dissipate in large concrete members, thus raising the concrete temperature significantly. Large internal stresses can be generated in the concrete because of the non-uniform temperature and stiffness development in the concrete members. Cracking can occur when the concrete residual stress exceeds the concrete tensile strength. A recent example of thermal cracking in a highway structure in Houston highlights the risk posed by thermal cracking. Figure 1 shows the vertical thermal cracks that were found in a column in this structure. By engineering and optimizing the construction methods and concrete materials used to control the concrete temperature and internal stress development, the risk of cracking can be substantially reduced.

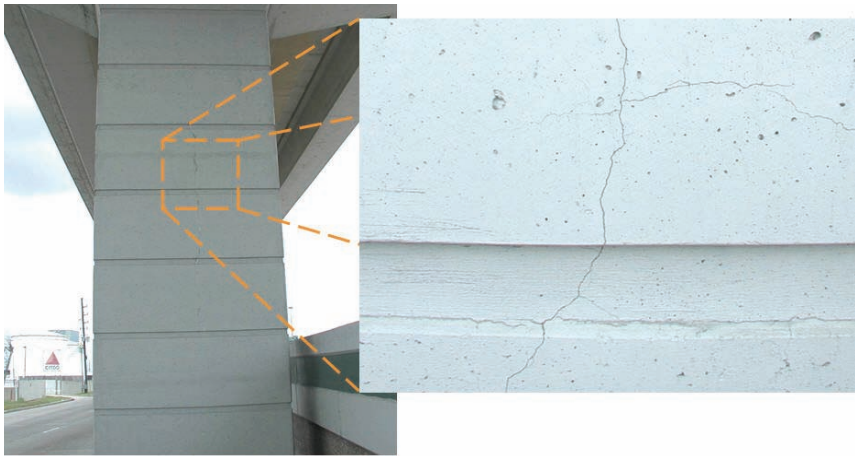

Figure 1.1 Thermal Cracking in a column in the IH-10 in Houston, TX (photo courtesy of J.C. Liu)

Thermal cracking in mass concrete elements has been recognized since the beginning of the twentieth century, when it was first discovered in dams (ACI 207 2005). Thermal gradients in bridge elements were generally not considered in the United States. Recently, however, more attention has been given to concrete bridge members as their size has grown in recent years because of structural and aesthetic reasons. The departments of transportation in the United States that have a mass concrete specification try to reduce the risk of concrete cracking indirectly by limiting the maximum temperature reached and maximum temperature difference in the concrete member (Chini et al. 2003). Owners and engineers in Europe, however, have chosen a more scientific approach for reducing the risk of thermal cracking in mass concrete. Large jobs in Europe (such as the Chunnel from England to France) conduct laboratory testing such as adiabiatic calorimetry and advanced cracking frame testing as well as perform a finite element thermal stress analysis prior to construction of a project (Poole 2007). It is not, however, cost-effective to perform a comprehensive laboratory analysis for every mass concrete member built by TxDOT. A model that can predict the heat of hydration and early-age mechanical property development of concrete based on the materials and mixture proportions has been developed as part of this research project. These material behavior models have been incorporated into ConcreteWorks to allow the user to quickly evaluate the member temperature development and consequent probability of thermal cracking.

1.1.2 Predicting Temperature and Heat Transfer

A model for predicting the temperature development in concrete members was developed and incorporated into ConcreteWorks. This model takes into account the heat generated by the hydration reaction, the heat transfer inside of the concrete member, and the interaction between the structure and its environment. Models were developed for quantifying the concrete heat of hydration based on the concrete materials used. First, the temperature sensitivity of the hydration reaction (described with activation energy, E_a) was needed to accurately predict the behavior of concrete under a variety of temperature conditions. A multivariate regression model was obtained from isothermal calorimetry testing to capture the effects of water-to-cementitious materials ratio (w/cm), cement chemistry, supplementary cementitious materials (SCMs), and chemical admixtures on the E_a of portland cement pastes. Next, a multivariate regression model was developed from semi-adiabatic calorimetry testing that predicts the heat generation rate and the total amount of heat released during hydration for different cementitious systems based on the mixture proportions, cement and SCM chemistry, and chemical admixture dosages. This model is presented in Chapter 2 of this report and in greater detail in the dissertation of Jonathan Poole (2007).

The heat transfer resulting from the interaction with the environment also needed to be quantified. The model includes components for calculating the radiation heat transfer components due to solar radiation, atmospheric radiation, ground surface radiation, radiation exchange with formwork bracing, and irradiation. The model also includes a method to characterize the effects of free convection, forced convection, and surface roughness. In addition, the impact of construction sequencing on the heat transfer and temperature of the members was developed. The model for all these effects is described in Chapter 3 of this report and in detail in Riding (2007).

1.1.3 Stresses and Failure Criteria

In order to assess the early-age cracking potential it is necessary to know the stresses that develop due to temperature and to set failure criteria. First, the mechanical property development in the concrete members was quantified. The equivalent age maturity method was used to address the effects of different temperatures on the mechanical property development. In ConcreteWorks, the concrete elastic modulus is calculated from the compressive strength in order to simplify the software inputs.

The concrete free deformation was also quantified in order to calculate a concrete member's restrained stress. A free shrinkage frame was developed to measure the free thermal and autogenous dilation of the concrete mixture (Riding 2007). The hardened concrete coefficient of thermal expansion (CTE) was also measured using a similar procedure to Tex-428-A, "Determining the Coefficient of Thermal Expansion of Concrete" (2001).

Cracking frame testing was used to obtain the early-age concrete stress relaxation, as described in Chapter 4. A non-linear multivariate model was developed that estimates creep compliance constants for a concrete mixture based on the concrete constituent material properties and mixture proportions.

Finally, accurate failure criteria were needed. Using tensile stresses at failure from the cracking frame tests, an equation relating tensile strength to compressive strength was developed. Thus, the user only needs to input compressive strength, and the program estimates the modulus of elasticity and the tensile strength from that value. The estimated tensile strength versus the predicted stress in the concrete (the strength to stress ratio) is what determines cracking potential. This is described further in Chapter 4.

1.2 Durability Problems

1.2.1 Delayed Ettringite Formation

For delayed ettringite formation (DEF) to occur, the concrete member must have a high internal temperature, and sufficient moisture must be available in the hardened concrete to allow for the formation of expansive ettringite (Famy 1999). The high temperatures inhibit the formation of ettringite and accelerate the formation of calcium silicate hydrate (C-S-H) during curing. The sulfate that would usually help form ettringite at normal temperatures is trapped by the rapidly forming C-S-H. Later in the life of the structure, the sulfate and aluminate ions absorbed by the C-S-H are released into the pore solution of the hardened cement paste to react with available monosulfate hydrate to form ettringite. This exerts pressure on the surrounding concrete, causing expansion and cracking (Famy 1999) as shown in Figure 1.2.

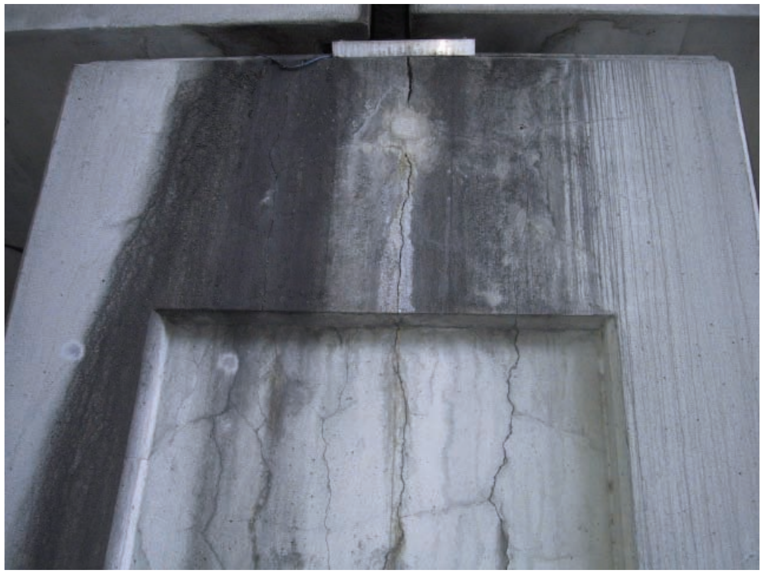

Figure 1.2 DEF in a column in San Antonio, TX

It is generally accepted that DEF can occur when the concrete, made with only portland cement, is subjected to temperatures of 158 °F (70 °C) or more during curing (Famy 1999). ConcreteWorks contains a module that will warn the user if the concrete temperature exceeds 158 °F (70 °C), which is a nominal temperature threshold above which DEF may occur. Although it has been shown that using suitable dosages of SCMs or lithium compounds can prevent DEF-induced expansion even when this temperature threshold is exceeded (Folliard et al., 2006), ConcreteWorks uses this specific maximum temperature value as a "red flag" for convenience.

1.2.2 Alkali-Silica Reaction

Alkali-silica reaction (ASR) expansion can occur when the aggregates in the concrete contain reactive silica, sufficient alkalis are present in the pore solution, and sufficient moisture is available in the hardened concrete (Hobbs 1988). Hydroxyl ions in the pore solution react with the reactive amorphous silica, forming a gel. The negatively charged species in the gel attracts positively charged alkalis from the pore solution. When sodium and potassium ions are incorporated into the gel, it can potentially absorb water and expand, causing cracking such as that shown in Figure 1.3. ASR is one of the most common concrete durability problems worldwide (Hobbs 1988).

Figure 1.3 ASR in a transmission tower foundation in La Grange, TX

ConcreteWorks checks the concrete mixture used for compliance with the prescriptive concrete mixture proportions options found in TxDOT Specification 421.4 (TxDOT 2004). This standard presents a number of options for mixture designs, such as replacing some cement with fly ash or ground-granulated blast-furnace (GGBF) slag, that are intended to help mitigate against ASR. If none of these options are fulfilled by the user of ConcreteWorks, the program will notify the user that the mixture does not comply with the TxDOT specification.

1.2.3 Chloride Ingress

The most common durability problem in structural concrete members is corrosion of the steel reinforcement. Chlorides can penetrate into the concrete at a slow rate through the interconnected pore structure in the concrete (Young et al. 1998). When a sufficient amount of chlorides penetrate the concrete to the steel reinforcement, the chlorides degrade the passive layer protecting the steel from corrosion. The corrosion products develop, causing large expansive stresses and cracking. Concrete spalling can then occur, further damaging the concrete structure. If the corrosion is allowed to progress further, the load-bearing capacity of the structure can be reduced enough to lead to a structural failure.

As described in more detail in the ConcreteWorks User Manual, ConcreteWorks contains a chloride diffusion service life model for mass concrete and bridge decks. As part of the chloride service life analysis, ConcreteWorks calculates the chloride concentration at the reinforcing steel depth. When the chloride concentration reaches the chloride threshold level, corrosion is considered to initiate. The propagation period for reinforcing bars is assumed to occur over a period of 6 years with standard reinforcing bars and immediately with prestressed strands. The service life model enables engineers to evaluate the lifespan of the concrete structure during the design process.

1.2.4 Sulfate Attack

Sulfate attack can occur when the concrete is exposed to sea water, sulfate containing groundwater or soil, or other industrial sources of sulfate (Young et al. 1998). If sulfate ions penetrate into the concrete, the dissolved sulfate ions may react with cement hydration products to form ettringite, resulting in expansion and cracking or in some cases loss of cohesion. An expansive force is created during the reaction with the sulfate ions, which causes internal stresses and cracking. Additionally, physical sulfate attack can occur when sodium sulfate ions penetrate into the concrete. Expansive pressures occur when the sodium sulfate changes phase during the diurnal temperature cycle (Young et al. 1998).

There are several things that can be done to prevent sulfate attack, such as lowering the w/cm, using sulfate-resistant cement, and using supplementary cementing materials (SCMs). It should be noted that the use of sulfate-resistant cement is only effective in reducing damage from chemical sulfate attack, not from physical sulfate attack. ConcreteWorks allows the user to specify the sulfate exposure level according to Table 4.3.1 of the ACI 318-05 building code, which enforces a maximum w/cm and minimum target strength requirements during the ACI 211 mixture proportioning guide module.

1.2.5 Freeze-Thaw

Damage due to freezing and thawing cycles can generally be avoided by using an air-entraining admixture. Freeze-thaw damage is not considered in the ConcreteWorks program.

2. Heat of Hydration

Most of the research presented in this chapter, as well as the models produced, are obtained from Poole (2007).

2.1 Introduction

While an in-depth thermal stress analysis is not typically done on highway projects in the United States, many mass concrete projects contain specifications limiting the temperature differential to 35° F (20° C) and the maximum internal temperature to 158° F (70° C) to control thermal cracking and delayed ettringite formation (DEF), respectively. Contractors are required to prove that any concrete deemed "mass concrete" meets these specifications. Unfortunately, even though the premises behind the specifications are well understood, the research behind the 35° F (20° C) specification is ambiguous. Data of measured temperature differentials to validate this criterion are limited, specifically since guidelines for instrumentation are vague. As a result, most thermal analyses of "smaller" mass concrete elements, like bridge structures, are inadequate. A better method is needed to estimate the temperature development in mass concrete elements.

The remainder of this chapter presents a model for concrete hydration, providing engineers with a cost-effective tool to estimate the in-place temperature development of different concrete mixtures in structures prior to placement. Thus, the risk of thermal cracking can be reduced by choosing concrete materials that will reduce the concrete heat of hydration. The model describes the effects of mixture proportions, cement and SCM chemistry, and chemical admixture dosages on the temperature sensitivity and adiabatic temperature rise of concrete. For a more detailed explanation of the model and the supporting research see the work of Poole (2007).

2.2 Method for Calculating the Apparent Activation Energy

During this study, isothermal calorimetry was performed on various cementitious pastes at 41° F (5° C), 59° F (15° C), 73.4° F (23° C), 100.4° F (38° C), and 140° F (60° C) using an eight channel isothermal conduction calorimeter. The calorimeter was kept in a temperature-controlled room at 70 ± 3° F (21 ± 2° C). Cement pastes were proportioned using a variety of w/cm. The water content was varied while the amount of cementing materials was held constant at 250 grams (0.55 pounds). Prior to mixing, materials were kept as close as possible to room temperature. Pastes were mixed in a kitchen blender for approximately three minutes. At higher w/cm, the mixture was re-agitated immediately preceding sample introduction into the ampoule so that the bleeding would not alter the w/cm of the paste in the ampoule. Eight tests were run simultaneously in the isothermal calorimeter. Each test sample had a mass of approximately 20 grams. Test durations ranged from 44 hours for those at 140° F (60° C) to over 100 hours for those at 40° F (5° C) in order to capture the rate of heat evolution during both the acceleration and deceleration stages of hydration at all temperatures tested.

The procedure used to calculate the apparent activation energy is a modified version of the ASTM C1074 method for calculating the activation energy from the compressive strength of mortar cubes cured at different isothermal temperatures. The concept of "equivalent age" (Freiesleben Hansen and Pederson 1977) is necessary to calculate E_a and to predict hydration behavior at various curing temperatures. Equation 2.1, proposed by Freiesleben Hansen and Pedersen (1977), is the most common expression used to compute equivalent age, and is used in the remainder of this chapter to model the effects of time and temperature on hydration:

$$t_e(T_r) = \sum_0^t e^{-\frac{E_a}{R}\cdot(\frac{1}{T_C}-\frac{1}{T_r})} \cdot \Delta t \tag{2.1}$$

where $t_e(T_r)$ = equivalent age at reference temperature (hr), T_r = reference temperature of the concrete (°K), T_C = temperature of the concrete (°K), and R = natural gas constant (8.314 J/mol/K).

In this derivation, E_a is assumed to be independent of temperature, which is consistent with the Arrhenius theory for rate processes. This is a reasonable approximation, given the relatively small temperature range concrete experiences in most situations.

The progress of the hydration of portland cement may be quantified by the degree of hydration (α), which varies from 0 to 1, with a value of 1 indicating complete hydration. For this study, degree of hydration is taken as the ratio of heat evolved at time, t, to the total amount of heat available, as shown in Equation 2.2 (Van Breugel 1998):

$$\alpha = \frac{H(t)}{H_u} \tag{2.2}$$

where α = degree of hydration at time t, $H(t)$ = heat evolved from time 0 to time t (J/gram), and H_u = total heat available for reaction (J/gram). The maximum heat of hydration (H_u) was calculated for the cements in this study using Equation 2.3 (Schindler and Folliard 2005):

$$\begin{aligned} H_{cem} &= 500 \cdot p_{C_3S} + 260 \cdot p_{C_2S} + 866 \cdot p_{C_3A} + 420 \cdot p_{C_4AF} \\ &+ 624 \cdot p_{SO_3} + 1186 \cdot p_{FreeCa} + 850 \cdot p_{MgO} \end{aligned} \tag{2.3}$$

where H_{cem} = total heat of hydration of portland cement (J/gram) at α = 1.0, and p_i = mass of i-th component to total cement content ratio.

A mathematical relationship may be used to model the degree of hydration development. Schindler (2005) suggested an exponential function to characterize cement hydration based on degree of hydration data. The most commonly used relationship is a three-parameter model defined in Equation 2.4 (Schindler and Folliard 2005):

$$\alpha(t_e) = \alpha_u \cdot e^{-\left[\frac{\tau}{t_e}\right]^{\beta}} \tag{2.4}$$

where t_e = equivalent age at reference temperature (T_r(°K)). This equation is explained in detail in Section 2.5.

The following equation (Schindler 2002) can be used to calculate E_a:

$$E_a = -\frac{\ln(\frac{\tau_{ref}}{\tau_c})}{(\frac{1}{T_{ref}} - \frac{1}{T_c})} \cdot R \tag{2.5}$$

where R = natural gas constant (8.314 J/mol/K), T_{ref} = reference temperature (K), T_C = temperature of the concrete (°K), τ = hydration time parameter (hours), and E_a as defined previously. A reference temperature (T_{ref}) of 73° F (22.8° C) is used for all activation energy calculations. The equivalent age is not determined when E_a is determined from the data collected from the isothermal calorimetry. An iterative process is thus not required. The steps to determine the activation energy are as follows:

- Time and heat evolution data from isothermal calorimeter tests are collected for the sample at different temperatures: 41° F, 59° F, 73° F, 100° F, and 140° F (5° C, 15° C, 23° C, 38° C, and 60° C) for this study.
- At each temperature solve for α_u, τ, and β using a least squares fit of the exponential function shown in Eq. 2.4. *Note time in this function is real-time, not equivalent age.* α_u and β are presumed independent of the test temperature.
- Plot ln(τ) versus 1/Temperature (°K). E_a is the slope of the best fit line, multiplied by the negative of the natural gas constant, *R*, which is defined in Eq. 2.5 as being equal to 8.314 J/mol/K.

2.3 E_a Trends

The first step in developing a model for E_a is to identify the trends that are visible without multivariate regression analysis. The results from isothermal calorimetry used to calculate E_a are presented by Poole (2007), and selected results will be discussed here to highlight several of the important trends that are apparent in the data. The following trends, summarized in Table 2.1, were identified from the results.

2.3.1 Cementitious Materials and w/cm

Increasing the C_3A or gypsum content of the cement increases E_a. In general, gypsum is added to cement to regulate the hydration of C_3A. Also, increased Blaine fineness decreases E_a. This is because the smaller particle size allows easier dissolution of the cement. Increasing w/cm slightly lowers E_a. The decrease is likely the result of dilution, since the increase in water content should promote the dissolution and hydration of the crystalline phases in the cement. A similar effect is seen with the addition of a low-CaO fly ash, since the reduction in reactive cement content in the system also effectively dilutes it with respect to water. It is also possible that the fly ash provides some preferential nucleation sites for C-S-H, increasing reactivity and thereby lowering E_a. However, the heat-of-hydration curves strongly suggest dilution as the primary mechanism.

2.3.2 Reactive Supplementary Cementitious Materials

The addition of reactive supplementary cementitious materials (SCMs) affects E_a in more complex manner than low-CaO fly ash does. Much of the sensitivity in E_a values when SCMs are used depends on the cement used in the system, i.e., trends that hold true for one cement may not hold for another. For some cements, the addition of ground-granulated blast-furnace (GGBF) slag or high-CaO fly ash raises E_a significantly, while for other cements, these SCMs have little effect. Silica fume reduces E_a fairly significantly. It is likely that the addition of silica fume to a mixture promotes the hydration of C_3S by providing preferential nucleation sites for C-S-H.

The specific effects of cement and SCM chemistry variables on E_a are difficult to parse. However, the ease with which the aluminate phase reacts seems crucial. Sulfate content and availability and alkalis strongly affect the hydration of the aluminates. E_a seems to be related to the total reactive aluminate phase in the system and its interaction with SCMs and chemical admixtures. SCMs or chemical admixtures that increase the height of the aluminate peak generally reduce E_a. Also, E_a seems to rise when the addition of highly reactive SCMs to the mixture does not substantially increase the height of the aluminate peak. Unfortunately, oxide analysis of the cement and SCMs only provides a part of the puzzle. Information on the availability of soluble sulfate, the phases in which the alkalis are present, and the reactivity of phases in the fly ash and GGBFS is not readily available, but may be important for a full understanding the hydration process.

2.3.3 Chemical Admixtures

Chemical admixtures have a variety of effects on E_a, as would be expected given their different effects on concrete performance. The addition of low-range water reducer (LRWR), water-reducer/retarder (WRRET), high-range water reducers (NHRWR and PCHRWR), and calcium nitrate-based accelerators (ACCL) reduce E_a to some degree. The addition of a retarder (WRRET) and an accelerator (ACCL) reduce E_a more than the other admixtures, and higher dosages of WRRET reduce E_a to a threshold value (Poole 2007). LRWR, HRWR, and PCHRWR act by dispersing and deflocculating cementing particles (either by ionic or steric repulsion). This facilitates the dissolution of the crystalline phases of the cement and tends to slightly reduce E_a. WRRET and ACCL affect the reaction rate and timing of the C_3S and C_3A in the cement, and tend to more greatly reduce E_a.

The data collected in this study suggest that the relationship between *WRRET* and E_a is nonlinear. With Cement C2 it was seen that E_a drops as *WRRET* dosage increases up to some limit of dosage. From previous research, dosages of *WRRET* over 0.35% by mass tend to excessively retard the cement paste, as reviewed by Poole (2007). When *WRRET* is overdosed, E_a ceases to drop. This type of relationship could be modeled by using a nonlinear equation. However, the dosage at which E_a ceases to drop may vary depending on the cement and SCM percentages in the mixture. Therefore, in the case of a very high dosage of admixture, a lower bound should be placed on the calculated value for E_a. It is suggested that a lower bound of 25,000 J/mol is appropriate until further testing can confirm the behavior of cementitious systems at extreme admixture dosages.

Table 2.1 Summary of Variables that affect E_a (Poole 2007)

Variable	Effect on E_a	Proposed Mechanism
Class F Fly Ash Replacement (↑)	↓	Dilution of cement with SCM
Class C Fly Ash Replacement (↑)	↔ for high C_3A, high Na_2O_{eq} cement;	Combination of SO_4^{2-} available to retard the aluminates and alkalis available to solubilize the SCM
	↑ for low C_3A, low Na_2O_{eq} cement	
GGBFS Replacement (↑)	↔ for High C_3A, high Na_2O_{eq} cement;	Combination of SO_4^{2-} available to retard the aluminates and alkalis available to solubilize the SCM
	↑ for Low C_3A, low Na_2O_{eq} cement	
Silica Fume Replacement (↑)	↓ for cement mixtures;	Dilution from SCM, nucleation sites for C_3S
	↓for mixtures with fly ash	
Higher w/cm	↓	Dispersion of cement from w/cm
Add LRWR	↓	Dispersion of cement by LRWR
Add HRWR	↓	Dispersion of cement by HRWR
Add WRRET	↓	Retardation of C_3S and acceleration of C_3A from WRRET
Add ACCL	↓ for cement mixtures;	Acceleration of C_3A and C_3S from ACCL
	↓ with fly ash replacement;	
	↔ with GGBFS replacement	
Add Alkalis to 0.85% Na_2O_{eq}	↔ for cement mixtures;	Solubility of reactive phases of fly ash goes up, which requires more SO_4^{2-} to regulate hydration.
	↑ with fly ash replacement	

2.4 Model for Estimating Activation Energy

The following models estimate the activation energy of cementitious systems. Based on the non-linear regression analysis mentioned above, two linear models were developed to describe the effects of different SCMs, admixtures, and cement properties. More specific details on these models, including the statistical analyses, can be found in Poole (2007).

2.4.1 Model using Bogue Calculations

The first model, based on phase analysis of the cement using Bogue calculations, uses independent variables that are readily available on mill certifications for cement, fly ash, slag, and silica fume. An analysis using Bogue compounds has inherent limitations. For example, the phases determined from Bogue calculations can be very inaccurate (Scrivener et al. 2004), especially when calculating C_3A. However, more complex phase analysis is often not available. The final form of the first model is shown in Equation 2.6 (Poole 2007):

$$\begin{aligned} E_a &= 41{,}230 + 8{,}330 \cdot \left[(C_3A + C_4AF) \cdot p_{Cement} \cdot Gypsum \cdot p_{Cement} \right] \\ &- 3{,}470 \cdot Na_2O_{eq} - 19.8 \cdot Blaine \\ &+ 2.96 \cdot p_{FlyAsh} \cdot p_{CaO-FlyAsh} + 162 \cdot p_{GGBFS} - 516 \cdot p_{SF} \\ &- 30{,}900 \cdot WRRET - 1{,}450 \cdot ACCL \end{aligned} \tag{2.6}$$

where p_{FlyAsh} = % fly ash in mixture; $p_{CaO\text{-}FlyAsh}$ = % CaO in fly ash; p_{GGBFS} = % GGBFS in mixture; p_{SF} = % silica fume in mixture; *Blaine* = Blaine fineness of cement; Na_2O_{eq} = % Na_2O_{eq} in cement (0.658 × %K_2O + %Na_2O); C_3A = % C_3A in cement; C_4AF = % C_4AF in cement; *Gypsum* = % gypsum in cement; *WRRET* = ASTM Type A&D water reducer/retarder, % solids per gram of cementitious material; *ACCL* = ASTM Type C calcium-nitrate based accelerator, % solids per gram of cementitious material.

2.4.2 Model using Rietveld Analysis

If Rietveld analysis of the cement is available, the second model is appropriate for the prediction of E_a, since it incorporates more accurate information about the aluminate and sulfate phases. The final form of the second model, based on Rietveld analysis, is shown in Equation 2.7 (Poole 2007):

$$\begin{aligned} E_a &= 39{,}200 + 107 \cdot \left[(C_3A) \cdot p_{Cement} \cdot (CaSO_4 \cdot xH_2O + K_2SO_4) \cdot p_{Cement} \right] \\ &- 12.2 \cdot Blaine + 1.24 \cdot p_{FlyAsh} \cdot p_{CaO-FlyAsh} + 120 \cdot p_{GGBFS} - 533 \cdot p_{SF} \\ &- 30{,}100 \cdot WRRET - 1{,}440 \cdot ACCL \end{aligned} \tag{2.7}$$

where $CaSO_4 \cdot xH_2O$ = sum of % by mass of gypsum, hemihydrates, and anhydrite, K_2SO_4 = % by mass of arcanite, and C_3A = % C_3A in cement, and all other variables are the same as for Equation 2.6.

2.5 Semi-Adiabatic Testing

Semi-adiabatic calorimetry is commonly used to provide an estimate of the heat generation characteristics of a concrete mixture because of the relative simplicity of the test. Semi-adiabatic calorimeters differ from adiabatic calorimeters in that they allow a small amount of heat loss from the system. Insulation is used to slow down the rate of heat loss. The amount of heat loss is measured, and the measured temperature values of the concrete are corrected to account for this loss. Then, the results are corrected to back-calculate the temperature rise that would occur under fully adiabatic conditions.

2.6 Calculation of Adiabatic Temperature Rise

The calculation of the adiabatic temperature rise of a concrete mixture is an iterative process. To provide the proper background, the governing equations will be discussed briefly. These equations are used to calculate fully adiabatic temperature rise. The equations for $t_e(T_r)$, α, and H_{cem} are calculated using Equations 2.1, 2.2, and 2.3.

Once again, Equation 2.4 is used to calculate $\alpha(t_e)$:

$$\alpha(t_e) = \alpha_u \cdot e^{-\left[\frac{\tau}{t_e}\right]^{\beta}}$$

where $\alpha(t_e)$ is the degree of hydration at equivalent age t_e. The parameters α, τ, and β model the shape of the hydration curve. They capture the effects of different mixture constituents on the amount of acceleration, retardation, rate of hydration, and degree of hydration of a mixture. τ, the hydration time parameter (hours), corresponds to the timing of the accelerating portion of the hydration curve. B, the hydration shape parameter, provides an indication of the rate of hydration. α_u, the ultimate degree of hydration, correlates with the total amount hydration. The way α, τ, and β affect the shape of the hydration curve are displayed in Figures 2.1, 2.2, and 2.3, respectively.

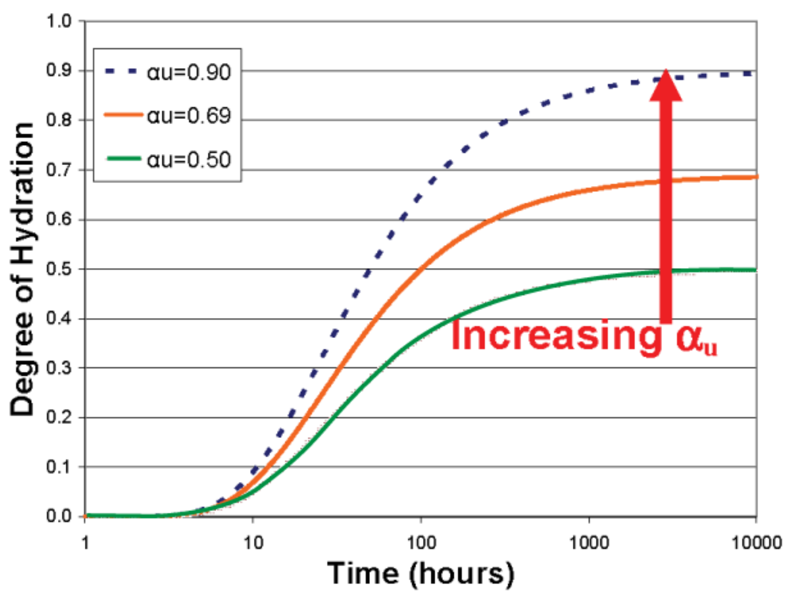

Figure 2.1 Effect of Increasing α_u on the Hydration Curve

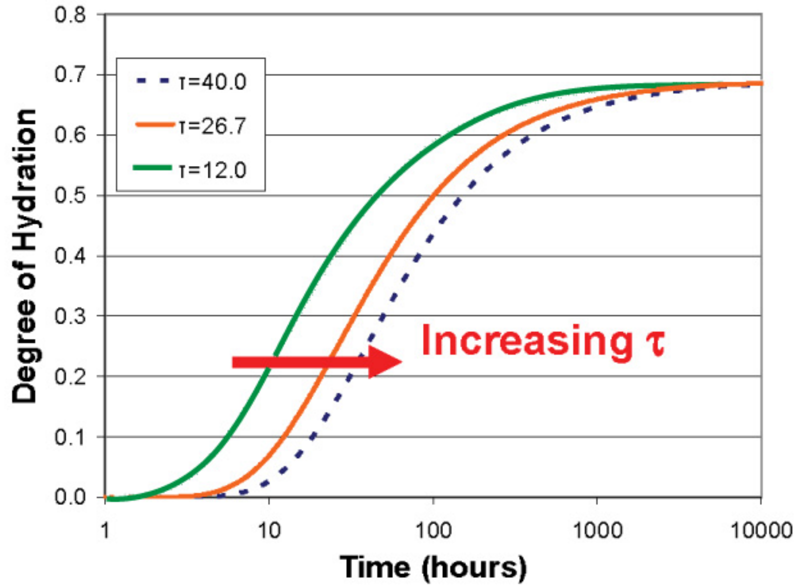

Figure 2.2 Effect of Increasing τ on the Hydration Curve

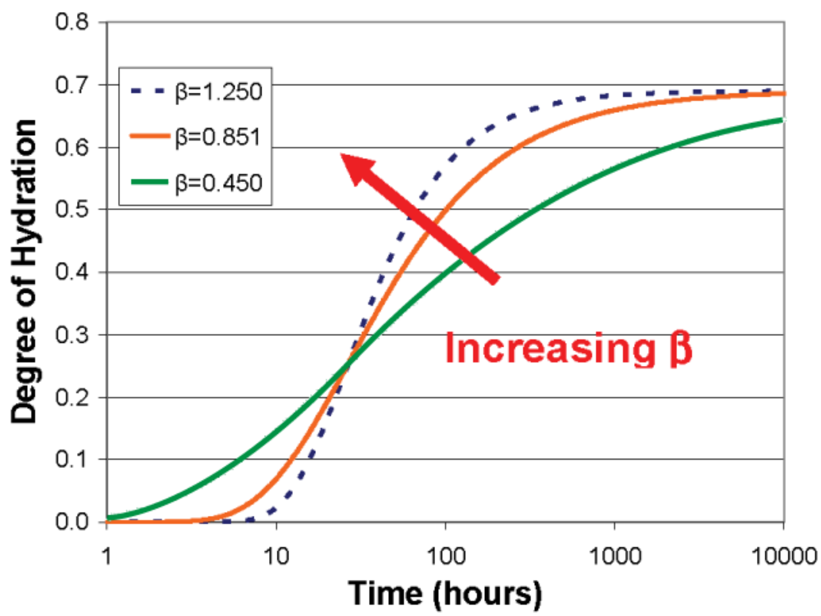

Figure 2.3 Effect of Increasing β on the Hydration Curve

A multivariate regression model for these parameters has been developed from semi-adiabatic calorimetry testing that takes into account mixture proportions, cement and SCM chemistry, and chemical admixture dosages. Figure 2.4 shows the isothermal and semi-adiabatic calorimeters used in the present study.

Figure 2.4 Isothermal Calorimeter (Left) and Semi-Adiabatic Calorimeter with Concrete Sample (Right)

H_u, the total heat available for reaction in J/gram, is a function of cement composition and amount and type of supplementary cementing materials (SCMs) and may be calculated using Equation 2.8 (Schindler and Folliard 2005):

$$H_u = H_{cem} \cdot p_{cem} + 461 \cdot p_{slag} + 1800 \cdot p_{FA-CaO} \cdot p_{FA} \tag{2.8}$$

where p_{slag} = ratio of slag mass to total cementitious content, p_{FA} = ratio of fly ash mass to total cementitious content, $p_{FA\text{-}CaO}$ = ratio of fly ash CaO mass to total fly ash content, p_{cem} = ratio of cement mass to total cementitious content, and H_{cem} = heat of hydration of the cement (J/gram).

The rate of heat evolution of concrete can be calculated using Equation 2.9. Heat evolved at time t is as follows (Schindler and Folliard 2005):

$$Q_h(t) = H_u \cdot W_c \cdot \left(\frac{\tau}{t_e}\right)^{\beta} \cdot \left(\frac{\beta}{t_e}\right) \cdot \alpha(t_e) \cdot \exp\left(\frac{E_a}{R}\left(\frac{1}{273+T_r} - \frac{1}{273+T_c}\right)\right) \tag{2.9}$$

where Q_h= rate of heat generation (W/m^3), H_u = total heat available (J/kg), and W_c = cementitious materials content (kg/m^3). Equations for H_u are available in literature, but a more accurate equation is presented in this report, as will be discussed in Section 2.8. E_a, the apparent activation energy as presented in Section 2.4, describes the temperature sensitivity of the hydration reaction. A multivariate regression model from isothermal calorimetry testing was developed to describe the effects of w/cm, cement chemistry, SCMs, and chemical admixtures on the E_a of portland cement pastes. This model was presented in Section 2.4. The model is also discussed in detail in work by Poole (2007).

The fully adiabatic temperature rise is calculated using the following steps:

1. Perform a calibration test on the specific semi-adiabatic calorimeter.
2. Run a semi-adiabatic calorimeter test. The concrete temperature, heat flux out of the calorimeter, and time are recorded at 15 minute intervals.
3. Determine the apparent activation energy (E_a) of the mixture from isothermal calorimetry (Poole et al. 2007). E_a is used to determine the equivalent age (t_e) of the mixture at each time step.
4. Calculate t_e at each time step (every 15 minutes) using Equation 2.1.
5. Calculate the heat evolved at each time step with Equations 2.2-2.4 and 2.8-2.9.

6. Determine the heat lost through the calorimeter, and add the heat back to the heat generated in the test.
7. Calculate curve fit parameters α_u, τ, and β as shown in Equation 2.5. These are determined iteratively by comparing a theoretical semi-adiabatic curve (calculated with the three-parameter model, and accounting for heat loss from the specimen) with the actual temperature results from the calorimeter.
8. Calculate the adiabatic temperature rise ("false" adiabatic temperature rise) based on the temperature and heat loss data from Step 1.
9. Calculate the adiabatic temperature rise ("true" adiabatic temperature rise) based on the model parameters developed in Step 7.

2.7 Hydration Trends

As part of the development of a hydration model of concrete, over 300 semi-adiabatic tests were performed on a variety of different concrete mixtures. Poole (2007) examined the effects of cement type, SCM type and replacement percentage, and admixture type and dosage. Selected results are discussed here, and summarized in Table 2.2. These mixtures were used to develop a multivariate statistical model of hydration of concrete. Other mixtures were used to assess the variability of the test method developed.

2.7.1 Effects of SCMs on Hydration

Several trends observed pertaining to hydration behavior of different mixtures are summarized in Table 2.2. The composition of cement plays a role in the hydration parameters, but changes in SCM type, replacement percentage, and the use of chemical admixtures generally alter the degree of hydration more than the cement composition. For example, values of τ for all cements ranged from 9.3 hours for Type III cement to 15.0 hours for Type V cement, with an average value of approximately 12.0 hours. The slope parameter, β, had a range from 0.68 to 0.92 for all cement types. For comparison, the addition of GGBF slag raised τ from 25 to 45 hours and lowered β from 0.75 to 0.45. The addition of SCMs and chemical admixtures had a greater effect on the behavior of the mixture and tended to magnify the differences between cements.

The chemistry and type of fly ash greatly affect the hydration of a mixture. Previous studies (Schindler and Folliard 2005) showed that fly ash tends to retard set time, depending on the amount of reactive phases in the fly ash. Fly ash is currently classified in these modeling efforts only by the CaO content, which does not capture the subtleties of the variations between fly ash hydration characteristics. However, CaO content does provide an index of the hydraulicity of the material and may be used as a rough comparison between ashes. Research performed under this project has shown that low-CaO fly ashes tend to reduce the heat of hydration of the mixture primarily through dilution of the portland cement (Poole 2007). They reduce the slope of the accelerating portion of the hydration curve as well. Higher CaO fly ashes also reduce the heat of hydration, but show some hydraulic properties beyond pure dilution of the portland cement. They reduce the slope of the accelerating portion of the hydration curve and they increase the duration of the induction period of the mixture (Schindler and Folliard 2005).

Several other SCMs were tested as part of this study. Only one grade of GGBF slag (Grade 120) was incorporated in the calibration dataset of the model, which does not provide enough information to draw conclusions about the mechanisms caused by different GGBF slag chemistries and finenesses. However, the results provide enough information to comment on the general trends seen with GGBF slag. GGBF slag reduces the rate of heat evolution of a mixture, reduced the slope of the accelerating portion of the hydration curve, and increased the induction period, just like the high-CaO fly ash. It should be noted that two different types of Grade 120 GGBF slag were tested, and four additional GGBF slags were included in the validation dataset. Also, ultra-fine fly ash and silica fume were tested as binary systems and in ternary blends. The addition of silica fume slightly increased the peak of the rate of hydration. Ultra-fine fly ash affected hydration like the parent Class F fly ash from which it was derived.

2.7.2 Effects of Chemical Admixtures on Hydration

A variety of chemical admixtures were tested. An ASTM Type A low-range water reducer (LRWR) generally had a small effect on the hydration parameters, while a Type B&D low-range water reducer/retarder (WRRET) increased both τ and β substantially. An ASTM Type C accelerator (ACCL) decreased τ. Also, most of the admixtures tested tended to increase β and decrease α_u. However, LRWR, WRRET, and ACCL tended to show some interaction with SCMs, which makes modeling of the various hydration parameters difficult.

Table 2.2 Effect of Different Mixture Characteristics on Exponential Model Hydration Parameters

Variable	Range of Tests	Effect on τ	Effect on β	Effect on α_u
Fly Ash (%Replacement)	15-55%			
Fly Ash (CaO%)	0.7-28.9% CaO			Varies
GGBF slag	30-70%	Large	Small	Varies
Silica Fume	5-10%	None	None	Small
LRWR	0.22-0.29%	Varies	Small	Varies
WRRET	0.18-0.53%	Large	Large	Large
MRWR	0.34-0.74%	Large	Small	Varies
HRWR	0.78-1.25%	None	Small	Small
PCHRWR	0.27-0.68%	None	Small	Small
ACCL	0.74-2.23%	Small	None	Varies
AEA	0.04-0.09%	None	None	None
Increasing w/c	0.32-0.68	None	None	Large
Placement Temp	50-100° F (15-38° C)	None	None	None
Increase Cement Fineness	350-540 m^2/kg	Small	Small	Varies

2.8 Model for the Hydration of Cementitious Systems

The following model estimates the degree of hydration of cementitious systems. First, a more accurate formula for the total heat available for reaction was developed. Based on the results of this study, Equation 2.8 should be modified as shown in Equation 2.10:

$$\begin{aligned} H_u &= H_{cem} \cdot p_{cem} + 461 \cdot p_{GGBF-100} + 550 \cdot p_{GGBF-120} \\ &+ 1800 \cdot p_{FA-CaO} \cdot p_{FA} + 330 \cdot p_{S.F.} \end{aligned} \tag{2.10}$$

where $p_{GGBF\text{-}100}$ = ratio of Grade 100 blast furnace slag (GGBF slag) to total cementitious content; $p_{GGBF\text{-}120}$ = ratio of Grade 120 blast furnace slag (GGBF slag; and $p_{S.F.}$ = ratio of silica fume to total cementitious content, and all other variables are as previously defined in Equation 2.8.

Non-linear regression analysis was performed on the calibration dataset for two cases. Two models are presented that describe the progress of hydration of concrete as characterized by the heat evolved. The first model uses commonly available information about the cementitious materials in the concrete mixture through oxide analysis and Bogue calculations. The second model is based on more precise information about the cementitious materials available from quantitative x-ray diffraction methods (Rietveld Method). Both models account for the effects of cement chemistry, aggregate type, w/cm, SCMs, chemical admixture type and dosage, and temperature on hydration.

2.8.1 Model using Bogue Calculations

The first case used cement crystalline phases determined from oxide analysis and Bogue calculations, and the results for α_u, τ, and β are shown in Equations 2.11 through 2.13 (Poole 2007).

$$\alpha_u = \frac{1.031 \cdot w/cm}{0.194 + w/cm} + \exp\begin{pmatrix} -0.885 - 13.7 \cdot p_{C_4AF} \cdot p_{cem} \\ -283 \cdot p_{Na_2O+0.658*K_2O} \cdot p_{cem} \\ -9.90 \cdot p_{FA} \cdot p_{FA-CaO} \\ -339 \cdot WRRET - 95.4 \cdot PCHRWR \end{pmatrix} \tag{2.11}$$

$$\tau = \exp\begin{pmatrix} 2.68 - 0.386 \cdot p_{C_3S} \cdot p_{cem} + 105 \cdot p_{Na_2O} \cdot p_{cem} + 1.75 \cdot p_{GGBF} \\ -5.33 \cdot p_{FA} \cdot p_{FA-CaO} - 12.6 \cdot ACCL + 97.3 \cdot WRRET \end{pmatrix} \tag{2.12}$$

$$\beta = \exp\begin{pmatrix} -0.494 - 3.80 \cdot p_{C_3A} \cdot p_{cem} - 0.594 \cdot p_{GGBF} \\ +96.8 \cdot WRRET + 39.4 \cdot LRWR + 23.2 \cdot MRWR \\ +38.3 \cdot PCHRWR + 9.07 \cdot NHRWR \end{pmatrix} \tag{2.13}$$

where p_{C3S} = % C_3S in cement, as determined by Bogue calculations, p_{C3A} = % C_3A in cement, as determined by Bogue calculations, p_{C4AF} = %C_4AF in cement, as determined by Bogue calculations, p_{Na2O} = %Na_2O in cement, $p_{Na2O+0.658 \cdot K2O}$ = % Alkalis as Na_2O, p_{cem} = % cement in mixture, p_{GGBF} = % blast furnace slag (GGBF slag) in mixture, p_{FA}=%fly ash in mixture, $p_{FA\text{-}CaO}$ = %CaO in fly ash, $p_{S.F.}$ = % silica fume in mixture, *ACCL* = accelerator, *WRRET* = ASTM Type B&D water-reducer/retarder, *LRWR* = ASTM Type A water reducer, *MRWR* = mid-range water reducer, *NHRWR* = ASTM Type F naphthalene or melamine-based high-range water reducer. All SCM dosages are percent replacement by mass of cementitious material. All admixture dosages are percent solids (by weight) per mass of cementitious material.

2.8.2 Model using Rietveld Analysis Techniques

The second case used cement crystalline phases as calculated by Rietveld analysis of x-ray diffraction data (Scrivener et al. 2004). Variables for each model were chosen so that only the method of cement analysis changed. The results based on Rietveld data for α_u, τ, and β are shown in Equations 2.14 through 2.16, respectively (Poole 2007):

$$\alpha_u = \frac{1.031 \cdot w/cm}{0.194 + w/cm} + \exp\begin{pmatrix} -0.297 - 9.73 \cdot p_{Ferrite} \cdot p_{cem} \\ -325 \cdot p_{Na_2O+0.658*K_2O} \cdot p_{cem} \\ -8.90 \cdot p_{FA} \cdot p_{FA-CaO} \\ -331 \cdot WRRET - 93.8 \cdot PCHRWR \end{pmatrix} \tag{2.14}$$

$$\tau = \exp\begin{pmatrix} 2.95 - 0.972 \cdot p_{Alite} \cdot p_{cem} + 152 \cdot p_{Na_2O} \cdot p_{cem} + 1.75 \cdot p_{GGBF} \\ -4.00 \cdot p_{FA} \cdot p_{FA-CaO} - 11.8 \cdot ACCL + 95.1 \cdot WRRET \end{pmatrix} \tag{2.15}$$

$$\beta = \exp\begin{pmatrix} -0.418 - 2.66 \cdot p_{Aluminate} \cdot p_{cem} - 0.864 \cdot p_{GGBF} \\ +108 \cdot WRRET + 32.0 \cdot LRWR + 13.3 \cdot MRWR \\ +42.5 \cdot PCHRWR + 11.0 \cdot NHRWR \end{pmatrix} \tag{2.16}$$

where p_{Alite} = % C_3S in cement, as determined by Rietveld analysis, $p_{Aluminate}$ = % C_3A in cement, as determined by Rietveld analysis, $p_{Ferrite}$ = % C_4AF in cement, as determined by Rietveld analysis, p_{Na2O} = % Na_2O in cement, $p_{Na2O+0.658 \cdot K2O}$ = % Alkalis as Na_2O, p_{cem} = % cement in mixture, p_{GGBF} = % blast furnace slag (GGBF slag) in mixture, p_{FA}=%fly ash in mixture, $p_{FA\text{-}CaO}$ = %CaO in fly ash, $p_{S.F.}$ = % silica fume in mixture, *ACCL* = accelerator, *WRRET* = ASTM Type B&D water-reducer/retarder, *LRWR* = ASTM Type A water reducer, *MRWR* = mid-range water reducer, *NHRWR* = ASTM Type F naphthalene or melamine-based high-range water reducer, and *PCHRWR* = ASTM Type F polycarboxylate-based high-range water reducer. All SCM dosages are percent replacement by mass of cementitious material. All admixture dosages are percent solids (by mass) per mass of cementitious material.

3. Temperature Modeling

ConcreteWorks is a user-friendly concrete mixture proportioning, thermal analysis, and chloride diffusion service life software package that was developed as part of this research project. The software package contains modules for several mass concrete shapes, bridge decks types, precast concrete beams, and concrete pavements. The following chapter briefly describes the process used to predict the heat transfer and temperature. Details of a comparison between measured temperatures of concrete members in the field and the temperatures predicted by ConcreteWorks can be found in the paper "Temperature Boundary Condition Models for Concrete Bridge Members (Riding et al 2007)." The information presented in this chapter is largely based on the ConcreteWorks User Manual (Riding 2007).

3.1 Basics of Temperature Prediction

The temperature development of mass concrete elements is dependent on constituent materials and mixture proportions, as well as geometry, formwork type, and environmental conditions (Riding 2007). These variables serve as inputs in the program. Thus, heat transfer and temperature prediction of a concrete member involves a number of interrelated mechanisms, none of which has a closed-form solution. Each of these mechanisms must be modeled, and a solution determined iteratively. The analysis consists of three main components: the heat conduction in the concrete, the heat generation from the hydration process, and the heat exchanged at the boundary of the structural element (Riding 2007). The modeling of these components is described in Sections 3.1.2 through 3.1.4.

3.1.1 Fundamentals of the Model

To simplify temperature prediction, control volumes are used (Figure 3.1). The temperature and material properties are assumed to be constant for each control volume. Sufficiently small control volumes must then be used to adequately approximate the heat transfer for each volume.

The heat transfer in real concrete members is much too complex for direct solutions, so numerical approximations are used to estimate the concrete temperature development. One such method is the finite difference method. An energy balance on an assumed differential control volume can be used to account for all thermal energy changes inside the control volume, as shown in Equation 3.1:

$$E_{in} - E_{out} + E_{gen} = \Delta E_{st} \tag{3.1}$$

where E_{in} (W) is the thermal energy entering the control volume, E_{out} (W) is the thermal energy leaving the control volume, E_{gen} (W) is the thermal energy being generated in the control volume (in the case of concrete, the heat generated by hydration), and ΔE_{st} (W) is the change in thermal energy stored in the control volume. The energy entering and leaving the control volume by conduction is equivalent to the first two terms in the heat diffusion equation. The heat generation term is the chemical energy being released in the control volume. The change in heat energy being stored in the control volume is equal to the change in temperature in the control volume times the specific heat and density.

To calculate the temperature in a node, the temperature variation with time needs to be assumed. Since it is impractical to predict the temperature continuously with respect to time,

time steps are used. The model used in ConcreteWorks features fully explicit time discretization, in which the temperature at the start of the each time step is assumed to be equal to the ending temperature of the pervious time step. Thus, the temperature increase over the time step can be calculated assuming the temperature state of the previous time step. This method is advantageous in that the unknown temperatures for the next time step do not have to be solved simultaneously.

However, if care is not taken when fully explicit methods are used, unstable results may be calculated (Riding 2007). In order to satisfy stability criteria, shorter time steps are required. The ConcreteWorks source code implements sufficiently small time steps, to satisfy the criteria for stability.

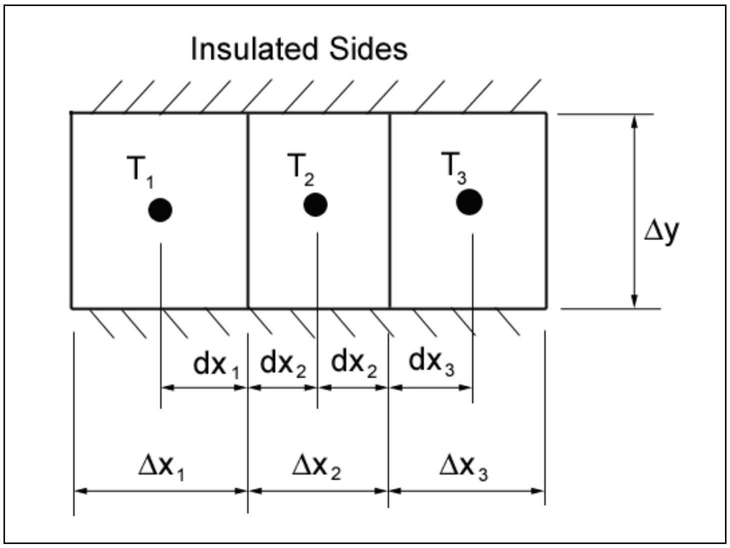

Figure 3.1 Control Volume Example - Three Neighboring Nodes (Riding 2007)

3.1.2 Concrete Conduction

Because of the constantly changing early-age properties of concrete, the concrete thermal properties must be updated at every time step. The thermal conductivity is known to be a function of "the moisture content, content and type of aggregate, porosity, density and temperature" (Van Breugel 1998). The concrete thermal conductivity increases with increasing moisture content. Though the conductive properties of concrete are well covered in literature, there is conflict about the change in thermal conductivity with increasing hydration. Based on the recommendation of Schindler (2002), ConcreteWorks assumes a linear decrease of the thermal conductivity with the degree of hydration from 1.33 times the ultimate thermal conductivity to the ultimate thermal conductivity as shown in Equation 3.2:

$$k_c(\alpha) = k_{uc} \cdot (1.33 - 0.33 \cdot \alpha) \tag{3.2}$$

where k_c is the concrete thermal conductivity (W/m/K), α is the degree of hydration, and k_{uc} is the ultimate hardened concrete thermal conductivity. The thermal conductivity of the concrete is not adjusted for moisture content in ConcreteWorks because the moisture content in mass concrete does not change significantly during early-ages. The thermal conductivity is also not adjusted for temperature.

The model used in ConcreteWorks for the specific heat of concrete, proposed by Van Breugel (1998), accounts for changes in the specific heat based on degree of hydration, mixture proportions, and temperature. Specific heat of concrete is calculated as follows:

$$C_p = \frac{1}{\rho} \cdot (W_c \alpha C_{ref} + W_c \cdot (1-\alpha) \cdot C_c + W_a C_a + W_w C_w) \tag{3.3}$$

where C_p = specific heat of concrete mixture (J/kg), ρ = unit weight of concrete (kg/m^3); W_c, W_a, W_w = amount by weight of cement, aggregate, and water (kg/m^3); C_c, C_a, C_w = specific heat of cement, aggregate, and water (J/kg/°C), and C_{ref} = specific heat of hydrated cement = $8.4 \times T_c + 339$ (J/kg/°C).

3.1.3 Heat of Hydration

The heat generated from the hydration process can be described by Equation 2.9. The concrete heat of hydration parameters H_u, τ, β, α_u, and E_a can be calculated based on the concrete mixture proportions and constituent material properties as explained in Chapter 2. The cement composition can be defined in ConcreteWorks using either the Rietveld method (Scrivener et al. 2004) determined from quantitative x-ray diffraction or the Bogue method calculated according to ASTM C 150 (2005).

The apparent activation energy E_a can also be calculated based on the cementitious material properties and the chemical admixtures used. Formulas for both the Rietveld and Bogue methods for the τ, β, α_u parameters were developed from a statistical analysis as described in Chapter 2. In addition, the H_u parameter can also be calculated from the cement chemical composition using a model developed by Schindler and Folliard (2005) and later altered to better characterize the influence of Grade 120 ground granulated blast furnace slag by Poole (2007).

3.1.4 Boundary Conditions

In calculating the heat transfer of concrete members, the boundary conditions are usually the most difficult parameters to quantify. ConcreteWorks makes numerous assumptions about the heat sources and sinks that are external to the concrete, depending on the user inputs. For example, the temperature prediction model contains weather files for 239 U.S. cities. These data files are applied to heat transfer calculations based on what city is chosen by the user.

Figure 3.2 illustrates the different radiation and convection surface boundary conditions from the environment to the outside formwork of a column. Radiation may be defined as "energy emitted by matter that is at a finite temperature" (Incropera and DeWitt 2002). Radiation exchange with the environment involves both incoming and outgoing components. Solar radiation, radiation from the atmosphere, radiation from the surrounding surfaces, and radiation from the formwork bracing are all heat sources and can all impact the surface temperature of the concrete. Irradiation, radiation emitted by the formwork, and reflected radiation act as heat sinks (Riding 2007).

Heat is transferred from the concrete surface to the surrounding air or water by convection. Convection involves energy transport by diffusion (random fluid particle motion contacting the surface) and bulk motion of the fluid. Convection transfer on the concrete surface consists of free and forced convection. Free convection is the heat transfer due to bulk fluid movement caused by buoyancy forces from the temperature differences in the air during heat exchange, and diffusion of the fluid (air or water) around the member. Forced convection is the heat transfer from bulk fluid movement caused by the wind (Riding 2007).

The finite difference method, described by Equation 3.1, allows for the treatment of each boundary condition effect separately at each time step (Incropera and DeWitt 2002). There are numerous equations needed to model each type of heat source or sink in ConcreteWorks. Details about the boundary condition equations used in ConcreteWorks may be found in work by Riding (2007).

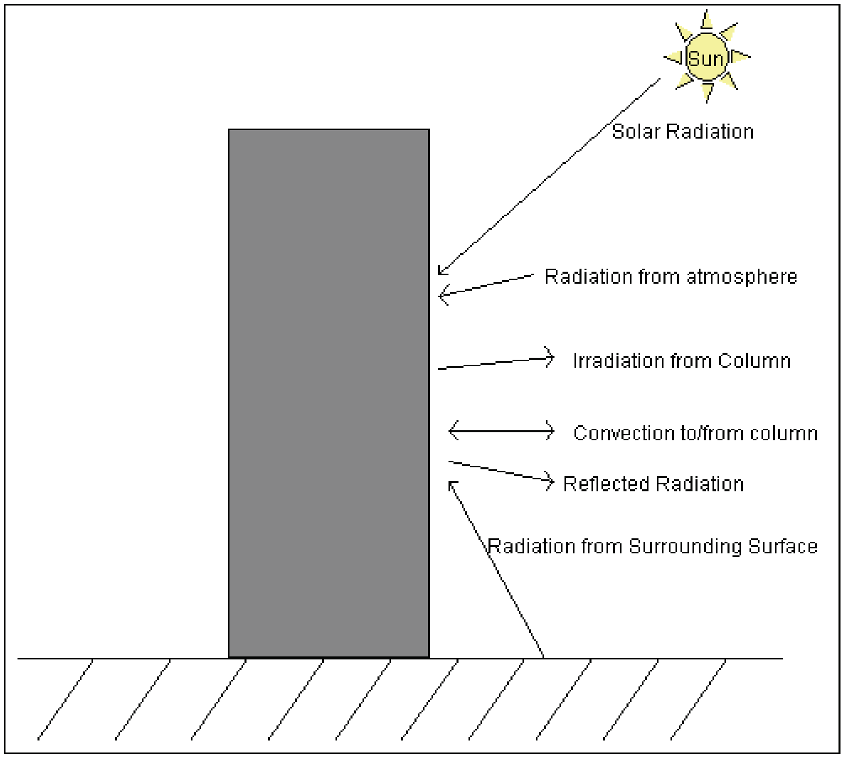

Figure 3.2 Summary of Column Boundary Conditions (Riding 2007)

3.2 Concrete Member Models

Each type of concrete member modeled in ConcreteWorks could have different formwork, boundary conditions, geometry, and opportunities to use symmetry. Temperature prediction is done differently with each type of member. For example, the boundary conditions of columns (Figure 3.2) differ from those of footings in that the boundary conditions for footings also include conduction to and from the soil. Types of members available in ConcreteWorks include variations of columns, footings, bent caps, drilled shafts, beams, bridge decks, and pavements. Different nodal arrangements are also required to keep nodes in a regular pattern and in-line. As an example, Sections 3.2.1 and 3.2.2 detail the geometry and construction stages involved in the temperature modeling of a rectangular column.

3.2.1 Geometry

ConcreteWorks makes use of the geometry of different structural elements to simplify the temperature model. It models a 2D horizontal cross-section for rectangular columns. The column heat transferred in the vertical direction is assumed to be zero, which is a reasonable assumption except near the top and bottom ends of the column. Other elements are modeled with a different cross-section. For example, bent caps are modeled with a vertical cross section.

The use of symmetry can significantly decrease the computational time needed, and is taken advantage of in ConcreteWorks. At a line of symmetry, the derivative of the temperature profile is theoretically zero. This implies that there is no heat exchanged across the line of symmetry. The energy leaving and entering the face of the control volume on the line of symmetry is set equal to zero. The assumption of symmetry may lead to some inaccuracies when modeling boundary conditions, such as when one side of a concrete member is shaded and the other is not. If symmetry were not assumed, longer run times would occur and more complex program inputs would be required (including inputs that may not be available to the engineer).

Rectangular columns are modeled using symmetry in both directions as shown in Figure 3.3. The formwork is handled by using half control volumes around the concrete, as shown in Figure 3.4. A “half control volume” is used for control volumes located on an external boundary (Patankar 1980) for more accurate modeling of the boundary condition effects. The conduction energy entering or leaving that side of the control volume can be replaced with the convection energy entering or leaving the control volume. As a result, the nodes of exterior control volumes are located at the interfaces of control volumes instead of in the center. Each type of member in ConcreteWorks is modeled geometrically in a unique manner that is used for producing sufficiently accurate results.

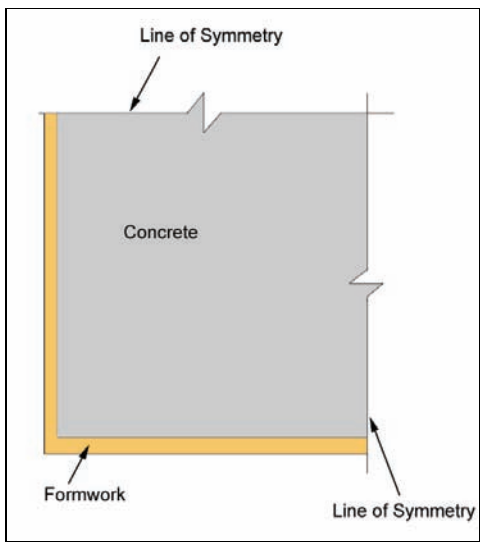

Figure 3.3 Simplified Rectangular Column Model used in ConcreteWorks (Riding 2007)

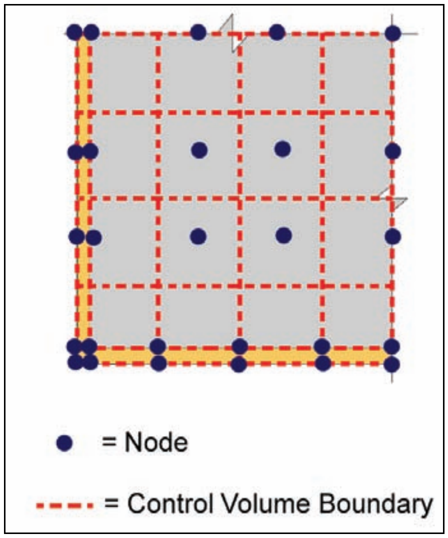

Figure 3.4 Example Rectangular Column Node and Control Volumes (Riding 2007)

3.2.2 Stages of Construction

The temperature of concrete members is modeled in ConcreteWorks according to different construction stages. The construction stages sometimes vary between different types of members to correctly represent construction methods used in the field. For rectangular columns, three construction stages are considered.

The first construction stage is during concrete placement and curing before form removal. When steel formwork is selected and form-liners are not selected, ConcreteWorks assumes that the steel provides no insulation because of the "little resistance to heat dissipation from the concrete" (ACI 207.2 1995). It is assumed that the surface of the formwork will still experience the same heating from the environment. When form-liners are used, ConcreteWorks calculates an equivalent form thermal conductivity, density, and specific heat for the selected combination of form and form-liner. The thermal conductivity, density, and specific heat of the equivalent form are calculated using equations found in Riding (2007).

The second construction stage modeled for rectangular columns is after form-removal and before curing techniques such as plastic, cure blankets, or cure compounds are applied. An example of a structure during the beginning of the second construction stage is shown in Figure 3.5. The formwork is virtually removed in ConcreteWorks by eliminating the formwork control volume, and applying boundary conditions such as convection and radiation directly to the surface concrete control volumes. Concrete emissivity, absorptivity, and surface roughness values are assigned at this point to the surface concrete control volumes.

Figure 3.5 Rectangular Column during Form Removal and the Beginning of the Second construction stage (Riding 2007)

Construction stage three for concrete columns is during the time period of concrete curing using blankets, curing compounds or plastic. When only curing compounds or only plastic are used, ConcreteWorks assigns the curing compound or plastic emissivity, absorptivity, and roughness values to the concrete surface control volumes. When curing compounds are used in conjunction with plastic or blankets, the effect of curing compounds is assumed to be negligible from a heat transfer point of view. When blankets are used but no plastic is used for curing, half control volumes (similar to those used for modeling the formwork) are applied to the exterior of the concrete control volumes. Blanket thermal and roughness properties are assigned to the exterior half control volumes. Blanket insulation properties are calculated from the blanket R-value entered by the user. The R-value is equivalent to the thickness divided by the thermal conductivity. When plastic and blankets are used to cure the concrete, blanket insulation properties (thermal conductivity, specific heat, density, and thickness) are assigned to the exterior half control volumes while the plastic emissivity, absorptivity, and roughness values of plastic are used.

3.3 Comparison with Field Site Data

Concrete temperatures for twelve structural elements of varying geometry, formwork, location, construction methods, and materials were predicted using the model described in this report (Riding, 2007). The concrete temperatures were predicted using the measured minimum and maximum weather data, instead of 30-year average weather data. This was done so that the predicted and measured concrete temperatures would not reflect the variation in the weather from the 30-year average weather values. The measured concrete hydration parameters obtained from semi-adiabatic calorimetry were also used in the analysis. Details about this study may be found in work by Riding (2007).

The value for each temperature sensor was compared to the predicted temperature. The maximum temperature and maximum temperature difference (the maximum difference between the maximum temperature and the minimum temperature anywhere in the concrete member) measured for each concrete member was compared to the predicted values, as shown in Table 3.1 and Table 3.2 (Riding 2007).

Table 3.1 Comparison of Predicted to Measured Maximum Concrete Member Temperature

Name of Member	Max. Temp Measured °F (°C)	Max. Temp Predicted °F (°C)	Difference in Max Temp °F (°C)
Pedestal	165.2 (74.0)	161.0 (71.7)	-4.1 (-2.3)
T-Shaped Cap	153.5 (67.5)	153.0 (67.2)	-0.5(-0.3)
Rectangular Bent Cap	128.3 (53.5)	127.0 (52.8)	-1.3 (-0.7)
Dolphin 1	145.4 (63.0)	149.2 (65.1)	3.8 (2.1)
Dolphin 2	149.9 (65.9)	149.9 (65.5)	0.0 (0.0)
Footing 1	145.4 (63.0)	142.0 (61.1)	-3.4 (-1.9)
Footing 2	133.0 (56.1)	135.2 (57.3)	2.2 (1.2)
Footing 3	147.2 (64.0)	141.1 (60.6)	-6.1 (-3.4)
Footing 4	135.0 (57.2)	135.0 (57.2)	0.0 (0.0)
Column 1	136.0 (57.8)	132.6 (55.9)	-3.4 (-1.9)
Column 2	163.4 (73.0)	169.9 (76.6)	6.5 (3.6)
Pilaster	130.1 (54.5)	125.8 (52.1)	-4.3 (-2.4)

Table 3.2 Comparison of Predicted to Measured Maximum Concrete Temperature Difference

Name of Member	Max. T Measured °F (°C)	Max. T Predicted °F (°C)	Difference in Max. T°F (°C)
Pedestal	43.2 (24.0)	36.5 (20.3)	6.7 (3.7)
T-Shaped Cap	65.7 (36.5)	54.2 (30.1)	11.5 (6.4)
Rectangular Bent Cap	27.9 (15.5)	30.1 (16.7)	2.2 (1.1)
Dolphin 1	72.0 (40.0)	72.5 (40.3)	0.5 (0.3)
Dolphin 2	55.8 (31.0)	57.2 (31.8)	1.4 (0.8)
Footing 1	38.7 (21.5)	34.0 (18.9)	4.7 (2.6)
Footing 2	23.4 (13)	22.1 (12.3)	1.3 (0.7)
Footing 3	41.4 (23.0)	36.2 (20.1)	5.2 (2.9)
Footing 4	41.4 (23.0)	37.4 (20.8)	4.0 (2.2)
Column 1	40.0 (22.2)	34.7 (19.3)	5.3 (2.9)
Column 2	60.3 (33.5)	54.4 (30.2)	5.9 (3.3)
Pilaster	65.7 (36.5)	59.8 (33.2)	5.9 (3.3)

The temperature model provides a good estimate of the maximum temperature in the concrete, with a maximum error of 4.9%. The model output differed by as much as 17.6% in predicting the maximum temperature difference in the concrete (Riding 2007).

The temperatures for Footings 1, 3, and Column 1; however, were predicted with less accuracy than other members. The prediction for column 1 was inaccurate because one of the exterior points did not correctly capture the magnitude of daily temperature fluctuations after the forms were removed. It is not known why Footings 1 and 2 showed inaccurate results. The concrete's heat of hydration in Footings 1 and 3 was not measured. Instead, the heat of hydration obtained from tests performed earlier on mixtures with the same mixture proportions, which could be the cause of the associated error (Riding 2007).

Some variation between measured and predicted temperature data is to be expected, due to rapid and short-lived temperature variations which occur in the microclimate surrounding the concrete members. The data analysis showed that the temperature prediction model, using average temperature data scaled for actual maximum and minimum values, provided an acceptable result when predicting the concrete temperature. In case of an extreme event such as snow, thunderstorms, or freezing, the reduction in accuracy is highly variable and depends on the magnitude and duration of the event. For this reason, these extreme events are not considered in the model (Riding 2007).

4. Development of Early-age Properties

Thermal stress modeling in concrete members is non-linear because of changing early-age material properties (elastic modulus, strength, Poisson's ratio, and coefficient of thermal expansion), differential temperature development, and creep. Figure 4.1 shows how the non-linear concrete property and restrained stress development can be calculated.

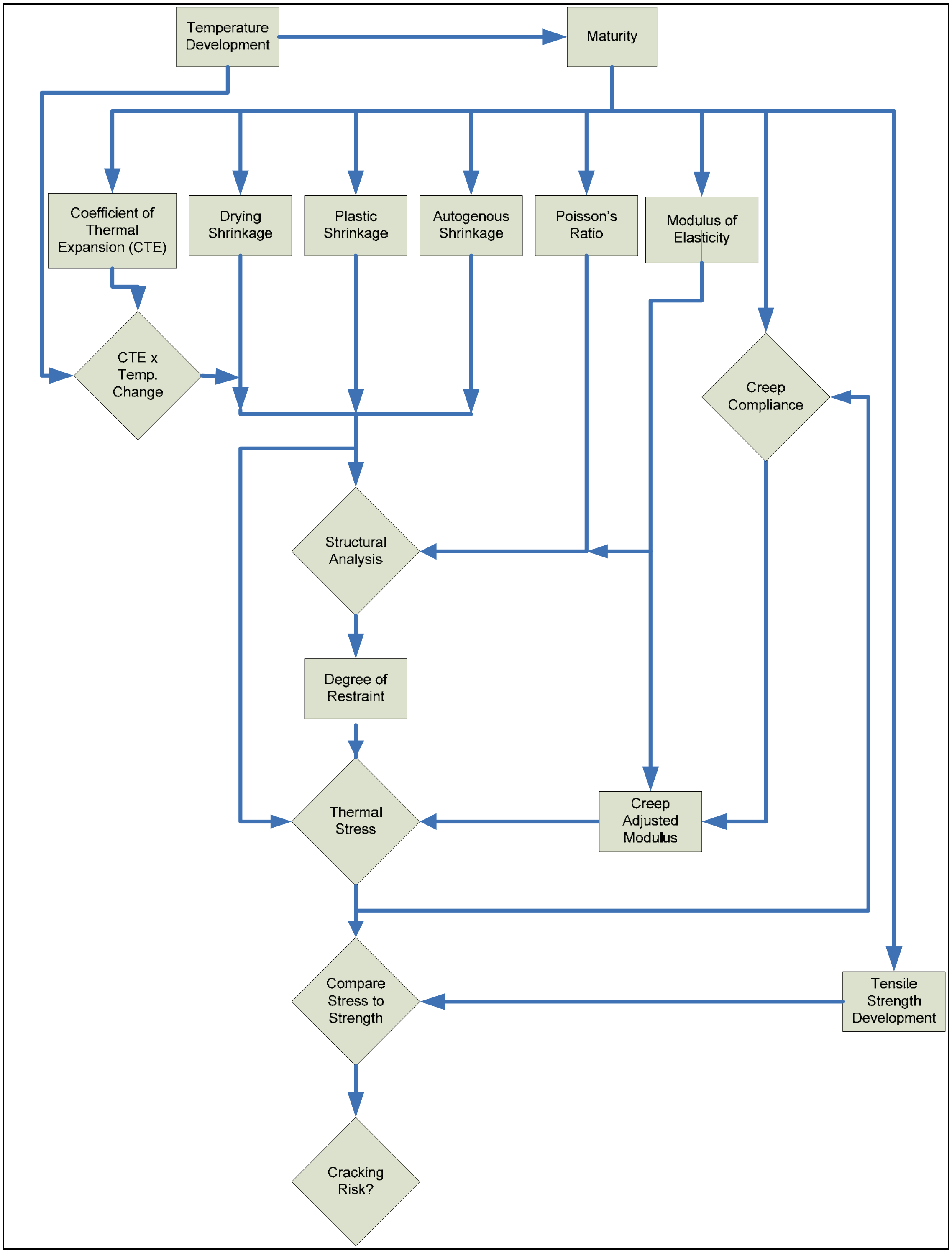

Figure 4.1 Flow chart describing the relationship between different parameters in thermal stress modeling of concrete structures (Riding 2007)

In order to calculate the thermal stresses, the concrete member degree of hydration and temperature development must first be calculated as described in Chapter 3. Next, the degree of hydration and temperature development is used to calculate the member mechanical properties and the strains the concrete would undergo if there were no restraint. These calculated values include the elastic modulus development, Poisson's ratio, tensile strength development, coefficient of thermal expansion, and autogenous and drying shrinkage. Next, the concrete elastic stress must be calculated from the free shrinkage strains and mechanical properties by performing a structural analysis. Stress relaxation may then be applied to the concrete elastic stress. Finally, a failure criterion such as the stress to tensile strength ratio may be used to determine the probability of cracking. The specifics behind these steps are provided in detail in the following sections.

4.2 Mechanical Property Development

In order to accurately model early-age stress development in concrete members, it was necessary to determine the development of mechanical properties (compressive strength, tensile strength, modulus of elasticity). The mechanical property development calculations used in ConcreteWorks are explained in detail in the ConcreteWorks User Manual (Riding 2007).

4.2.1 Maturity

The rate of cement hydration of specific cement is dependent on the temperature and the time since mixing (Mindess, Young, and Darwin 2003). Maturity is a method to account for the effect of curing temperature on the rate of hydration of the cementious materials. There are two maturity methods commonly used, both of which are described in ASTM C 1074 (2004). They are the Nurse-Saul method and the equivalent age method.

The Nurse-Saul method concept was developed first in the 1950s and uses a temperature-time factor to define maturity. The temperature-time factor may be defined as the integral of the temperature history (ASTM C 1074 2004). The equivalent age maturity is the age a concrete sample would have to be cured isothermally at some reference temperature T_r (°C) to have the same degree of reaction or properties as the sample cured at a different temperature (ASTM C 1074 2004).

ConcreteWorks uses the equivalent age maturity method because it better accounts for the effect of temperature on concrete strength development than the Nurse-Saul method (Emborg 1998; Mindess, Young and Darwin 2003).

4.2.2 Compressive Strength

A good model that describes the compressive strength development is essential in ConcreteWorks because it is used to calculate the elastic modulus development and the splitting tensile strength development. The compressive strength is the most widely used strength quality control test. Many engineers and contractors have already gained experience in developing compressive strength-maturity relationships, making it a much easier parameter for ConcreteWorks users to input than the modulus or splitting tensile strength to maturity relationship.

Many forms of equations have been developed to relate the compressive strength to the maturity development. Two commonly used equations are shown in Equations 4.1 and 4.2 (Viviani 2005):

$$f_c(t) = a + b \cdot \log(\log(M(t))), f_c \geq 0 \tag{4.1}$$

$$f_c(t_e) = f_{cult} \cdot \exp\left(-\left(\frac{\tau_s}{t_e}\right)^{\beta_s}\right) \tag{4.2}$$

where f_c is the compressive strength development (MPa), a is a fit parameter which is usually negative (MPa), b is a fit parameter (MPa/°C/hr), f_{cult} is the ultimate compressive strength parameter fit from the compressive strength tests (MPa), τ_s is a fit parameter (hrs), and β_s is a fit parameter. Equation 4.1 is not ideal for use in thermal stress analysis, because it is discontinuous at setting and has a different form to the model that best characterizes the development of hydration (Eq. 2.4). Equation 4.1 is only allowed to be used in ConcreteWorks when the Nurse-Saul maturity method is used.

4.2.3 Tensile Strength

The splitting tensile test does not measure the true tensile strength of the concrete. Small regions of compression are developed during the test, causing the true concrete tensile strength to be overestimated (ASTM C 496 2004; Mindess, Young and Darwin 2003). This study used the results of 64 restrained cracking frame tests and accompanying match-cured concrete cylinders to determine the ratio of stress-to-splitting tensile strength at cracking.

Though the splitting tensile test is the most commonly performed tensile strength test for concrete, it is not usually performed for actual projects (Riding 2007). The concrete tensile strength is usually estimated from its compressive strength. Most current methods of calculating splitting tensile strength assume a power type function based on the compressive strength, as shown in Equation 4.3 (Raphael 1984):

$$f_{ct} = a \cdot (f_c)^b \tag{4.3}$$

where f_{ct} is the concrete splitting tensile strength, a and b are fit parameters, and f_c is the concrete compressive strength.

For this project, a total of 743 tests of compressive and splitting tensile strength were performed. The power law relationship between the measured splitting tensile strength and the compressive strength shown in Equation 4.3 fit the data reasonably well. Fit parameters a and b were found to be 0.266 and 0.907, respectively with an R^2 of 0.95 (Riding 2007).

4.2.4 Modulus of Elasticity

The elastic modulus is also commonly calculated from the concrete's compressive strength. Most models of this type follow a form of Equation 4.4:

$$E = k \cdot (f_c)^n \tag{4.4}$$

where f_c is the compressive strength (MPa), and k and n are model parameters. ACI 318 (2005) uses a form of this equation where n is equal to 0.5 and k is as shown in Equation 4.5:

$$k = 0.043 \cdot w_c^{1.5} \tag{4.5}$$

where w_c is the unit weight of the concrete (kg/m^3). ConcreteWorks uses Equations 4.4 and 4.5 in calculating the elastic modulus from the compressive strength development. The default values set in ConcreteWorks are equal to those used in the ACI 318 building code. This equation was chosen because most engineers are familiar with this equation from prior experience in structural design, and readily accept its use. Most ConcreteWorks users will also not have test data available to model the elastic modulus development, making the use of readily accepted default equations necessary.

4.3 Free Shrinkage Device

A free shrinkage frame has been developed to measure the free thermal and autogenous dilation of the concrete mixture (Riding 2007). Figure 4.2 shows a diagram and picture of the free shrinkage frame. The free shrinkage specimen dimensions are 6" x 6" x 20.4" (150 x 150 x 520 mm). The bottom bar is made of Invar, as are the two threaded rods that are embedded in the concrete. The threaded rods are screwed onto linear potentiometers, which are then threaded onto 1" x 1" (25 x 25 mm) plates which are embedded in the concrete.

Layers of plastic are used between the concrete and the formwork, with a lubricant applied under each layer, to reduce friction between the specimen and the formwork. The copper pipes in the free shrinkage frame's formwork are connected in series with the cracking frame and circulator to ensure that the free shrinkage frame's temperature stays within about 1.8° F (1° C) of the temperature of the concrete in the rigid cracking frame. The temperature is recorded using two thermocouples.

The free shrinkage is initialized and set to zero at initial setting as determined following ASTM C 403 (2006). The samples for the setting test were also match-cured to the temperature history of the free shrinkage frame. The top surface is sealed with plastic and adhesive aluminum tape. The opening on the end plate is drilled larger than the rod to reduce friction between the rod and the plate when the rod moves. Grease is used to fill the remainder of the hole left by the threaded Invar rods to prevent moisture loss. The hole in the top formwork was drilled larger than the thermocouples to ensure that no restraint is provided by the thermocouple probes. Silicone is used to seal the holes in the formwork where the thermocouples are inserted.

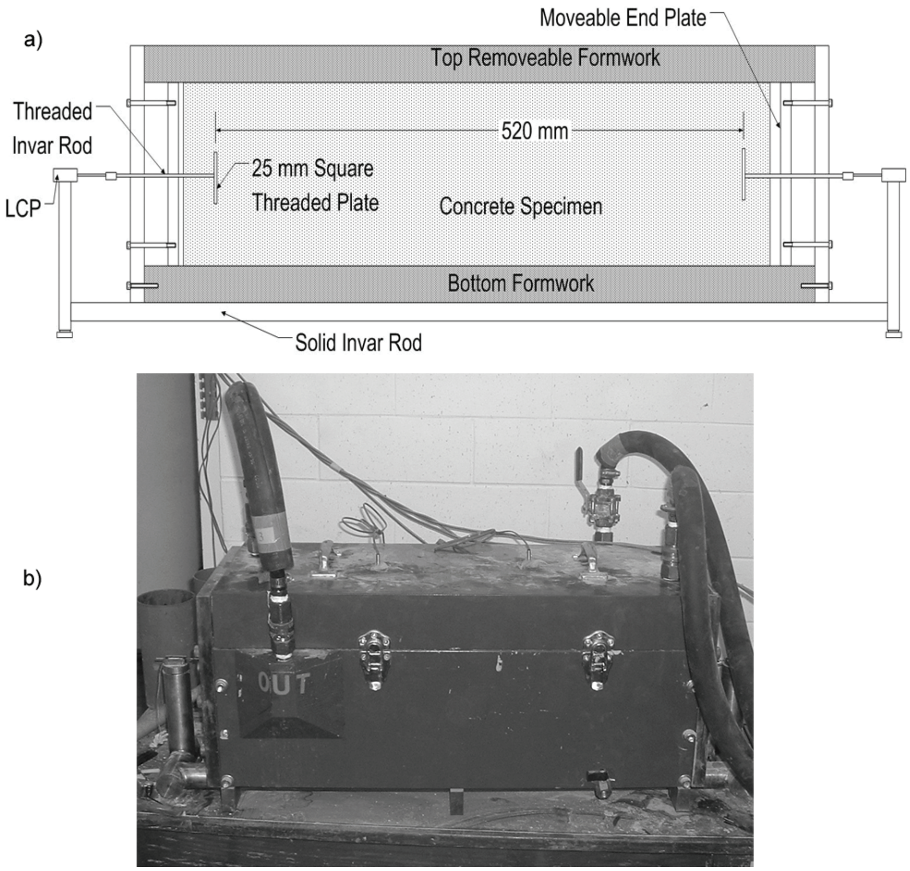

Figure 4.2 Free Shrinkage Frame a) Diagram and b) Frame used for this project

4.4 Cracking Frame Methodology

The concrete uniaxial stress under restrained conditions is measured using a rigid cracking frame (Mangold 1998). Figure 4.3 shows a drawing of the rigid cracking frame and Figure 4.4 shows a picture of the test setup (Riding 2007). A 6” x 6” x 49” (150 x 150 x 1250 mm) concrete specimen is placed, consolidated, and cured in the rigid cracking frame. The formwork of the rigid cracking frame allows the temperature of the freshly placed concrete to be conditioned to simulate various structural elements. The temperature of the rigid cracking frame specimen is controlled using a programmable refrigerating/heating circulator that circulates a 50/50 mixture of water and ethylene glycol through copper pipes in the formwork and cracking frame crossheads.

The main purpose of the crossheads is to grip the concrete so that the rigid Invar side bars restrain the concrete specimen against deformation (Whigham 2005). In order to prevent slippage of the test specimen, each crosshead contains two sets of teeth that grip the concrete. Preliminary testing in the cracking frame produced undesirable cracking in the crosshead that originated from the back of the first tooth. The sharp corners of the teeth produce localized stress concentrations. In order to alleviate the stress concentrations and prevent cracking in the crossheads, the back side of the first two teeth on each side of the crosshead was chamfered approximately 1/16” (1.59 mm). With this improvement, cracking at the crosshead only occurs when the concrete is improperly placed.

Packing plates secure the Invar bars to the crossheads (Whigham 2005). The circulator is controlled based on the temperature in the middle of cracking frame measured using a Type T thermocouple. The temperature in the concrete crossheads is also measured using Type T thermocouples. Because the temperature in the concrete is actively controlled, the difference between the temperature in the specimen middle and crosshead is generally within 0.9°F/hr (0.5°C/hr). If the concrete specimen does not crack after 96 hours, it is cooled at a rate of 1.8°F/hr (1°C/hr) to induce cracking in the concrete and to measure the direct tensile strength. The temperature at which the concrete cracks is referred to as the "cracking temperature" (Springenschmid and Breitenbücher 1998). The lower the cracking temperature, the better the concrete mixture resistance is to thermal cracking (Springenschmid and Breitenbücher 1998).

The stress in the rigid cracking frame is monitored with strain gauges mounted on the 3.94" (100 mm) diameter Invar restraining bars. These bars are designed to provide a high level of restraint while allowing small deformations that are measured with strain gauges (Whigham 2005). The restraining bars hold the crossheads 44" (1250 mm) apart. Invar has a very low coefficient of thermal expansion compared to mild steel. Invar is thus used for the bars to minimize thermal effects on the length change of the restraining bars.

The temperature of the Invar bars at the location of the strain gauges is measured using a resistance temperature detector (RTD) probe. The thermal movement of the Invar restraining bars also needs to be subtracted from the measured strain to calculate the actual stress induced strain in the Invar bars.

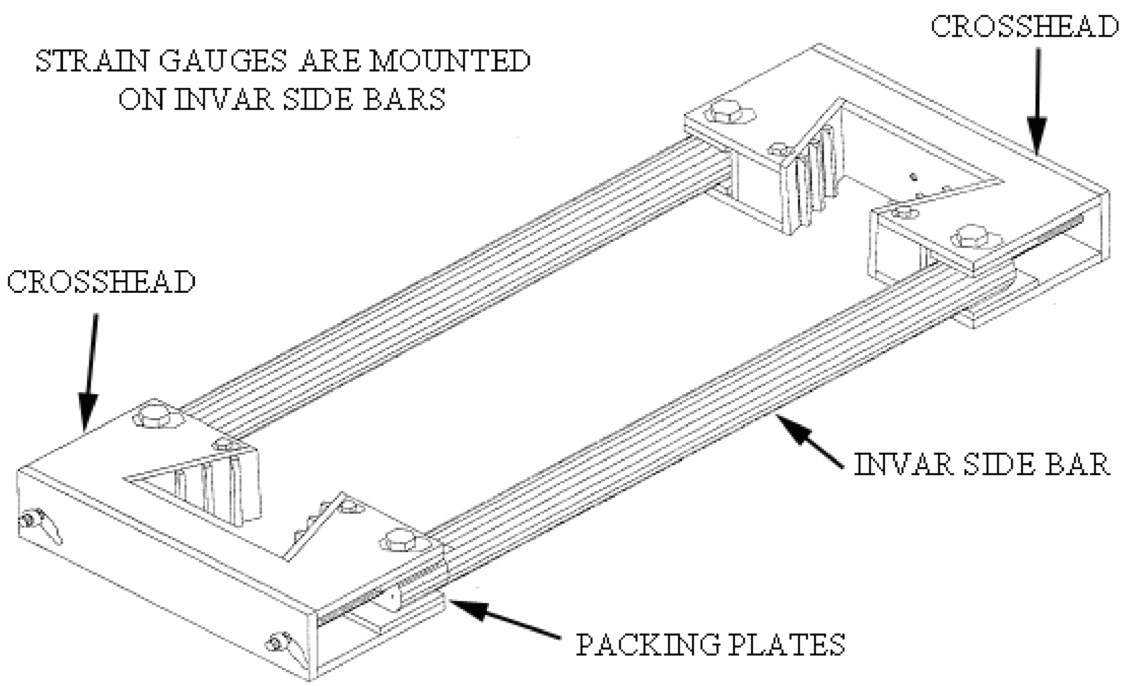

Figure 4.3 Rigid Cracking Frame Drawing

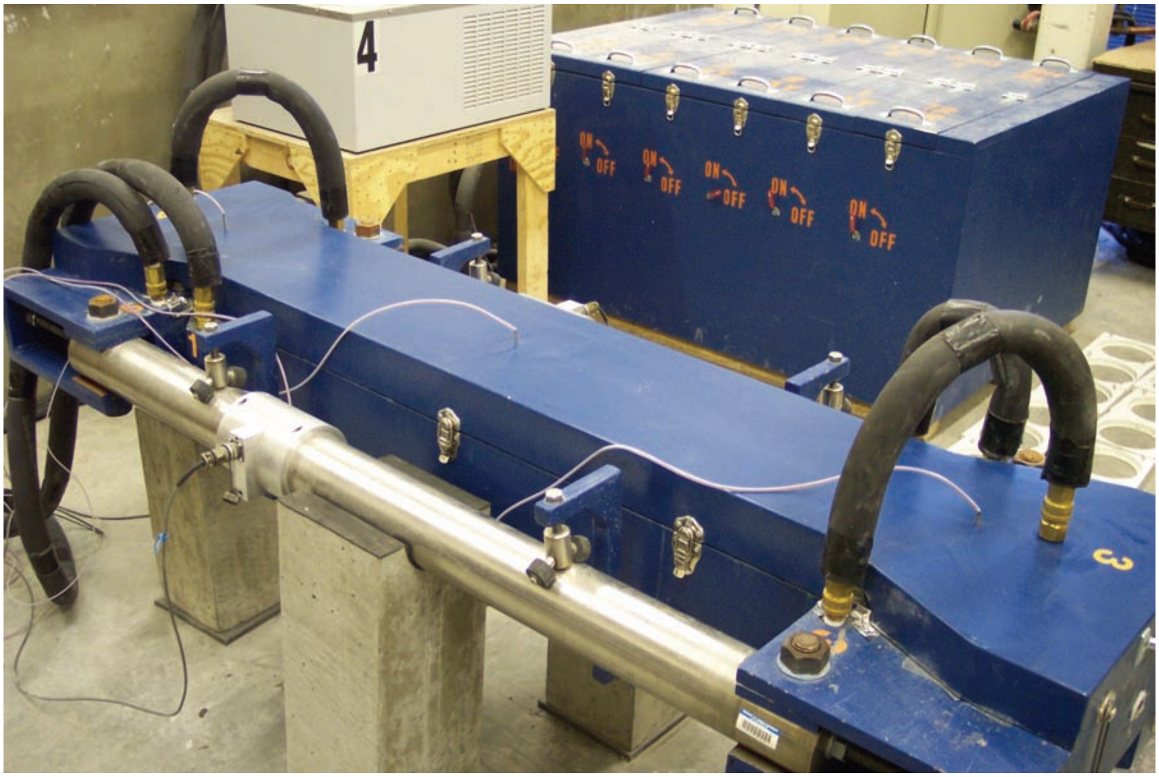

Figure 4.4 Photograph of Rigid Cracking Frame (Whigham 2005)

4.5 Creep Stresses

Restrained concrete tests can be used to measure the concrete early-age creep compliance (Altoubat 2000). The creep parameters can be adjusted to match the measured stress in the restrained concrete test (Riding 2007). The cracking frame procedure enables one to determine the stress development continuously from setting through hardening. As the concrete volume changes during hydration, the early-age concrete strain is restrained by the Invar side bars which convert a portion of the volume change into stress. The sealed concrete specimen can undergo early-age volume change because of autogenous shrinkage or thermal movement from the heat of hydration. The temperature of the concrete in the cracking frame may change due to the heat of hydration that is retained by formwork insulation, or it can be actively controlled using temperature controlled water that is circulated through copper pipes embedded in the formwork. The proportion of concrete deformation that is restrained from movement is called the degree of restraint and can be calculated using Equation 4.6:

$$\delta = \frac{100}{1+\left(\frac{E_c A_c}{E_s A_s}\right)} \tag{4.6}$$

where δ is the degree of concrete restraint, E_c is the concrete elastic modulus (MPa), A_c is the concrete cross sectional area (m), E_s is the Invar bar elastic modulus (MPa), and A_s is the Invar bar cross sectional area (m).

The strain gauges that are mounted on the Invar bars record the strain in the bars. The stress in the concrete can be obtained through a calibration process which involves correlating the frame stiffness to a known load applied with a hydraulic ram. The concrete stress is then corrected for strain in the Invar bar due to thermal movement of the Invar bar and strain gauge according to Equation 4.7:

$$\varepsilon_{Tadj} = \Delta T_{ib} \cdot \alpha_{ib} \cdot \delta \tag{4.7}$$

where ε_{Tadj} is the temperature induced strain of the Invar bar (m/m), ΔT_{ib} is the temperature change of the Invar bar at the strain gauge (°C), and α_{ib} is the coefficient of thermal expansion of the Invar bar (m/m/°C).

An exponential model first suggested by Freiesleben Hansen and Pedersen (1985) was used to model the concrete strength based on the concrete equivalent age maturity, as shown presented earlier in Equation 4.2. The static modulus of elasticity was then modeled based on the compressive strength development using Equation 4.5.

4.5.1 Modified Linear Logarithmic Method

The stress in the cracking frame was simulated using the measured modulus and strength values fit according to Equations 4.8 and 4.9 and calculated thermal and autogenous deformations for each of the rigid cracking frame tests performed. The simulation was performed for a period of 96 hours or until the concrete in the rigid cracking frame cracked, whichever came first. The creep parameters t_{a1}, t_{a2}, n_{a2} were iteratively changed until a good fit as measured by the coefficient of determination R^2 value was achieved. Tests at different temperatures were performed on the same concrete mixtures to investigate the effects of temperature on early-age concrete creep. When a concrete mixture was evaluated at several different temperatures, the same modified linear logarithmic model (MLLM) creep parameters were used to simulate that concrete mixture at all temperatures. This was done to facilitate early-age restrained stress modeling of structural members, in which the same creep parameters must be used to model the concrete stress development in all parts of the member, irrespective of the temperature history.

The modified linear logarithmic model creep parameters can be calculated with Rietveld data or Bogue data. A non-linear multivariate model was created that estimates the MLLM parameters for a concrete mixture based on the concrete constituent material properties and mixture proportions.

Equations 4.8 through 4.10 can be used to estimate the t_{a1}, t_{a2}, and n_{a2} MLLM creep parameters based on the Bogue method (Riding 2007):

$$t_{a1} = 0.728 + 0.0061 \cdot FA + 0.448 \cdot \ln(w/cm) - 0.0111 \cdot C_4AF \tag{4.8}$$

$$\begin{aligned} t_{a2} &= \exp(3.436 - 0.0179 \cdot (FA + GGBFS) - 3.404 \cdot w/cm \\ &\quad - 0.0186 \cdot C_2S - 0.0566 \cdot C_4AF) \end{aligned} \tag{4.9}$$

$$\begin{aligned} n_{a2} &= \exp(6.165 - 0.0541 \cdot FA - 0.0619 \cdot GGBFS - 0.00869 \cdot cement \\ &\quad - 0.425 \cdot C_3A - 0.572 \cdot C_4AF + 0.0107 \cdot CemBlaine) \end{aligned} \tag{4.10}$$

where C_4AF is the percent C_4AF of the cement, as calculated using the Bogue method, C_2S is the percent C_2S of the cement, as calculated using the Bogue method, C_3A is the percent C_3A of the cement, as calculated using the Bogue method, *cement* is the total amount of cementing materials used (kg/m^3), and *CemBlaine* is the cement Blaine fineness (m^2/kg). When a supplementary cementing material is used, the percent values used of the cement chemistry are the percent of the material in the cement times the percent cement of the total cementing materials. For example, the *perC*$_4$*AF* value used in the model of a concrete containing 30% SCMs and a portland cement containing 10% C_4AF would be 7%. The r^2 values for the Bogue model for the t_{a1}, t_{a2}, and n_{a2} parameters are 0.70, 0.69, and 0.77, respectively.

A separate non-linear multivariate model for calculating the MLLM creep parameters based on the Reitveld method has been created and is shown in Equations 4.11 to 4.13 (Riding 2007):

$$t_{a1} = 0.680 + 0.0064 \cdot FA + 0.429 \cdot \ln(w/cm) - 0.00965 \cdot Ferrite \tag{4.11}$$

$$\begin{aligned} t_{a2} = {} & \exp(3.671 - 0.0192 \cdot (FA + GGBFS) - 3.7169 \cdot w/cm - \\ & 0.10078 \cdot (Gypsum + Hemihydrate + Anhydrite + Arcanite) - \\ & 0.0556 \cdot Ferrite) \end{aligned} \tag{4.12}$$

$$\begin{aligned} n_{a2} = {} & \exp(-26.735 + 0.0705 \cdot FA + 0.072 \cdot GGBFS + \\ & 6.586 \cdot \ln(Alite) - 0177 \cdot Ferrite - 0.253 \cdot Alum + 5.194 \cdot w/cm) \end{aligned} \tag{4.13}$$

where *FA* is the percent fly ash replacement of cement by mass, *w/cm* is the water to cementing materials ratio, *Ferrite* is the percent ferrite of the cement, as determined by Rietveld analysis, *GGBFS* is the percent Grade 120 GGBF slag replacement of cement by mass, *Gypsum* is the percent gypsum of the cement, as determined by Rietveld analysis, *Hemihydrate* is the percent hemihydrate in the cement, as determined by Rietveld analysis, *Anhydrite* is the percent anhydrite in the cement, as determined by Rietveld analysis, *Alite* is the percent alite in the cement, as determined by Rietveld analysis, and *Alum* in the percent aluminate in the cement as determined by Rietveld analysis. The R^2 values for the Rietveld model for the t_{a1}, t_{a2}, and n_{a2} parameters are 0.70, 0.70, and 0.75, respectively.

4.6 Coefficient of Thermal Expansion (CTE) Testing

For obtaining the CTE for concrete mixtures, a procedure was carried out that is similar to the procedure designated by TxDOT, Tex-428-A (2001). The procedure used differed slightly, however, from the TxDOT standard method. The TxDOT method involves taking measurements and temperature readings every ten minutes over a thirty minute period. In the method used for this project, readings were taken only at the beginning and end of each temperature cycle once the temperature and the specimen length stabilized. The same level of accuracy in terms of temperature and length change was required. The method used proved to give almost exactly the same results as Tex-428-A. The coefficient of thermal expansion of the concrete was measured for each combination of aggregate types used in this study.

4.7 Cracking Frame Results

A total of 73 rigid cracking frame tests were performed on 36 different concrete mixtures. Several of the concrete mixtures were tested at different fresh concrete placement temperatures and different temperatures surrounding the simulated 1 meter thick wall. A few of the concrete mixture and temperature combinations were also repeated for quality control. A total of 9 cements, 6 different fly ashes, 1 Grade 120 ground granulated blast furnace (GGBF) slag, and 1 source of silica fume were evaluated in this study. Details of the mixtures and results can be found in work by Riding (2007).

The cement physical and chemical properties were determined using three different methods, the Blaine specific surface area (ASTM C 204 2005), the Rietveld method of quantitative x-ray diffraction (Scrivener et al. 2004), and the Bogue method specified in ASTM C 150 (2005) calculated from x-ray fluorescence.

Table 4.1 summarizes the effect of a change in each MLLM parameter on the concrete stress relaxation during the first 1-2 days of the simulations, and on the stress relaxation during days 2-4. Both the relative sensitivity of a change in each parameter and the direction of the change on the early-age stress relaxation are given in the table.

The use of GGBF slag during the first day slightly increased the early-age stress relaxation, but at later ages of between 1 and 4 days, decreased the concrete stress relaxation. The use of fly ash has a similar effect as GGBF slag on the concrete early-age stress relaxation, with an increased amount of stress relaxation before about 1-2 days which transitions to a decreased amount of stress relaxation after about 2 days. Grasley (2006) also found that fly ash increased the concrete early-age creep, and decreased the later age creep, with the transition occurring between 1 and 28 days. The similar early-age stress relaxation trends of fly ash and GGBF slag suggest that the same mechanism may be at work for both materials in reducing the later age creep. The increase in stress relaxation from the use of fly ash and GGBF slag can be attributed to the mainly slower rate of reaction of these materials. The decrease at later ages, however, can be attributed to a change in the structure and number of creep sites available, C-S-H stochastic ratios, and porosity of the C-S-H that may occur because of the pozzolanic reaction (Thomas and Jennings 2006).

Table 4.1 Effects of MLLM Parameters on Concrete Stress Relaxation (Riding 2007)

MLLM parameter	first 1-2 days	After the first 1-2 days
GGBFS		↓↓↓↓
Fly Ash		↓↓↓↓
w/cm		↓↓↓
Total Sulfates	↓	↓↓
Ferrite	↓↓	↓
Aluminate	↓↓	
Alite		↓↓
↑ = Increase in stress relaxation ↓ = Decrease in stress relaxation 4 arrows indicates a substantial change in the early-age stress relaxation, while 1 arrow indicates a minor change in the early-age stress relaxation		

4.8 Limitations

It should be noted, however, that there are several limitations to the model produced using the cracking frame results. The data set is limited to only 36 different concrete mixtures. The model is also limited based on the range of cement replacement levels with supplementary cementing materials. Larger cement replacements with supplementary cementing materials may affect the early-age hydration and consequently creep in unexpected ways. Additionally, the effects of admixtures such as shrinkage reducing admixtures have not been quantified as part of this study. This study did; however, test several concrete mixtures under widely varying temperature histories, allowing the model to be used as part of an early-age stress cracking probability analysis of members with non-uniform temperature developments.

The next obvious limitation of the model is that the rigid cracking frame simulations were only performed for a maximum of 96 hours. Any calculated creep response beyond 96 hours may give unreliable results. Additionally, the principle of superposition was used in the creep analysis which may lead to errors when the stress level is above 40% of the cracking stress (Westman 1999; Emborg 1998). This may be because of strain softening at higher compressive stress levels due to micro-cracking. Furthermore, at higher stress levels, the concrete may experience tertiary creep which can be very non-linear, violating one of the assumptions of the principle of superposition (Emborg 1998).

Even with the limitations discussed, the creep models outlined in this paper still provide a good estimate of the concrete early-age stress development. The 95% stress range of the simulated rigid cracking frame stress was within 71 psi (±0.49 MPa) of the measured rigid cracking frame stress values when using the Rietveld MLLM, and 74psi (±0.51 MPa) when using the Bogue MLLM. This implies that both the Rietveld and Bogue MLLM models may be used with good expected results.

4.9 Autogenous Shrinkage

The autogenous shrinkage modeling in ConcreteWorks is the best currently available; however, more work is required in this area. Autogenous shrinkage is currently predicted using the maturity concept. The maturity concept involves determining the time required for the cement paste to achieve the same level of development, at a certain temperature, as that under the effect of the actual time-temperature history (Turcry et al. 2002). However, actual autogenous shrinkage has proven to be dependent on temperature as well. Further research in this area is recommended.

5. ConcreteWorks

ConcreteWorks is designed to be a user-friendly concrete mixture proportioning, thermal analysis, and chloride diffusion service life software package. The software package contains design modules for several mass concrete shapes, bridge decks types, precast concrete beams, and concrete pavements. Table 5.1 shows the software analysis modules available for each member type.

Table 5.1 Software features available for each concrete member type (Riding 2007)

Member Type		Initial Chloride Profile Input for Existing Structures	Chloride Service Life	Thermal Cracking Risk	Temperature Prediction
Mass Concrete	Rectangular Column		X	X	X
	Rectangular Footing		X	X	X
	Partially Submerged Rectangular Footing		X	X	X
	Rectangular Bent Cap		X	X	X
	T-Shaped Bent Cap		X		X
	Circular Column		X		X
	Drilled Shaft		X		X
Precast Concrete Members	Box Beam (Type 5B40)				X
	Type IV I-Beam				X
	U40 Beam				X
	U54 Beam				X
Bridge Deck Types	Precast 1/2 Depth Panels	X	X		X
	Permanent Metal Decking	X	X		X
	Removable Forms	X	X		X
	User-Defined	X	X		X
Pavements	User-Selected Layers				X

In order to obtain accurate temperature, thermal stress, and corrosion risk predictions, the user should have a good understanding of the fundamental principles and mechanics employed in the software inputs and calculations. It is assumed that users will have a good knowledge of fundamental concrete materials principles and practices. The following chapter gives a brief explanation of how the program is used. Most of the following information is obtained from the ConcreteWorks User Manual (Riding 2007). The manual is designed to give the user a working knowledge of concrete behavior needed to successfully use ConcreteWorks, built upon an already existing knowledge of fundamental concrete behavior. It is recommended that users carefully read the user manual before using the software.

5.2 General Inputs

In ConcreteWorks, the user may select from four basic types of concrete members: mass concrete, bridge decks, pavements, or precast beams. Other inputs include the placement date, analysis duration, and project location. The “General Inputs” screen, shown in Figure 5.1, shows how easily a location in Texas can be selected by the user. The inputs in ConcreteWorks can be entered in either English units or Metric (S.I.) units. The English units system is the default system in ConcreteWorks.

The location chosen dictates the default environmental inputs. These inputs include the outdoor temperature, relative humidity, percent cloud cover, wind speed, and yearly temperature. The default inputs are obtained from the temperature prediction model, which contains weather files for 239 U.S. cities (Riding 2007). When using the program, the user should select the closest city to the construction site that has a similar climate. The default weather data can be altered, however. The relative humidity, wind speed, and dry bulb temperature used in the calculations can be scaled by the user by manually inputting maximum and minimum daily values. Solar radiation values can be adjusted indirectly by changing average daily cloud cover values (Riding 2007). Summary graphs are available as well. For example, the user can observe a graph of the ambient temperature versus time.

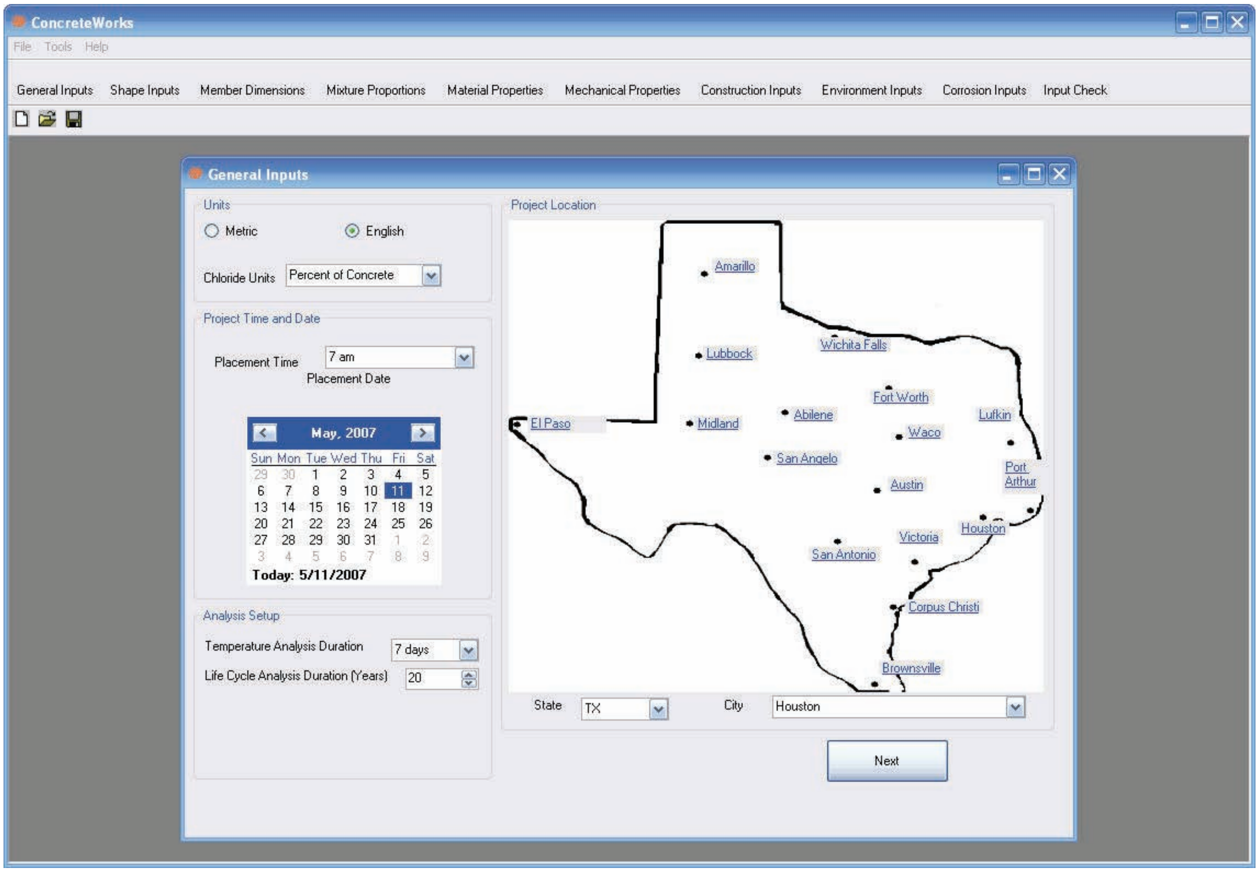

Figure 5.2 "General Inputs" Screen (Riding 2007)

Accurate results in ConcreteWorks depend on the user entering the correct time and date. Even if the minimum and maximum weather data are entered later in the program, the correct date and time must still be entered. The shape of the weather data plots are extracted from thirty-year average data. Because of the changing sunrise and sunset times, every day has a fundamentally different shape of the weather data plot. Entering the correct maximum and minimum weather data later in the program will give the correct overall magnitude for the weather data plots, but will not change the weather data's fundamental shape.

5.3 Member Geometry

The user inputs the member geometry. All the available shapes are shown in Table 4.1 in Chapter 4. The user inputs the cross-sectional dimensions of the member. Because the program's focus is on transportation related concrete (bridges and pavements), ConcreteWorks limits the size of some member dimensions. These limits are given in the ConcreteWorks User Manual (Riding 2007). Some members can be modeled as either submerged or with soil on the sides, such as an underwater column or a footing with clay or soil serving as the formwork.

Pavement analyses are broken up into different layers with different material properties. Users may select up to two types of subbase materials, in addition to the pavement and subgrade. The subgrade material is assumed to extend infinitely beneath the subbase layer(s). For footings, the user may decide whether to run a two-dimensional or three-dimensional analysis. Calculating the temperature in three dimensions can give slightly better results in some cases, but significantly increases the calculation run time.

5.4 Mixture Design

5.4.1 Mixture Proportions

After determining the geometry of the member, the concrete mix must be entered into the program, as seen in Figure 5.2. Mixture information is entered by the amount of weight of a particular material for every unit volume (pounds per cubic yard for English units, kilograms per cubic meter for SI units). The aggregate contents are entered assuming the aggregates are in a saturated surface dry (SSD) state. The water is entered based on total amount of free water available for hydration (aggregate moisture not absorbed + water/ice added).

The user can also select supplementary cementing materials (SCMs), to use in the mixture. With SCMs, the amount to be used in the batch must be specified. Chemical admixtures are entered by selecting the desired admixture. To simplify mixture proportion inputs, typical values of chemical admixture doses are assumed (see the User Manual (Riding 2007) for these assumed doses). Additionally, mixture ratios based on the current values entered are calculated and displayed to the user.

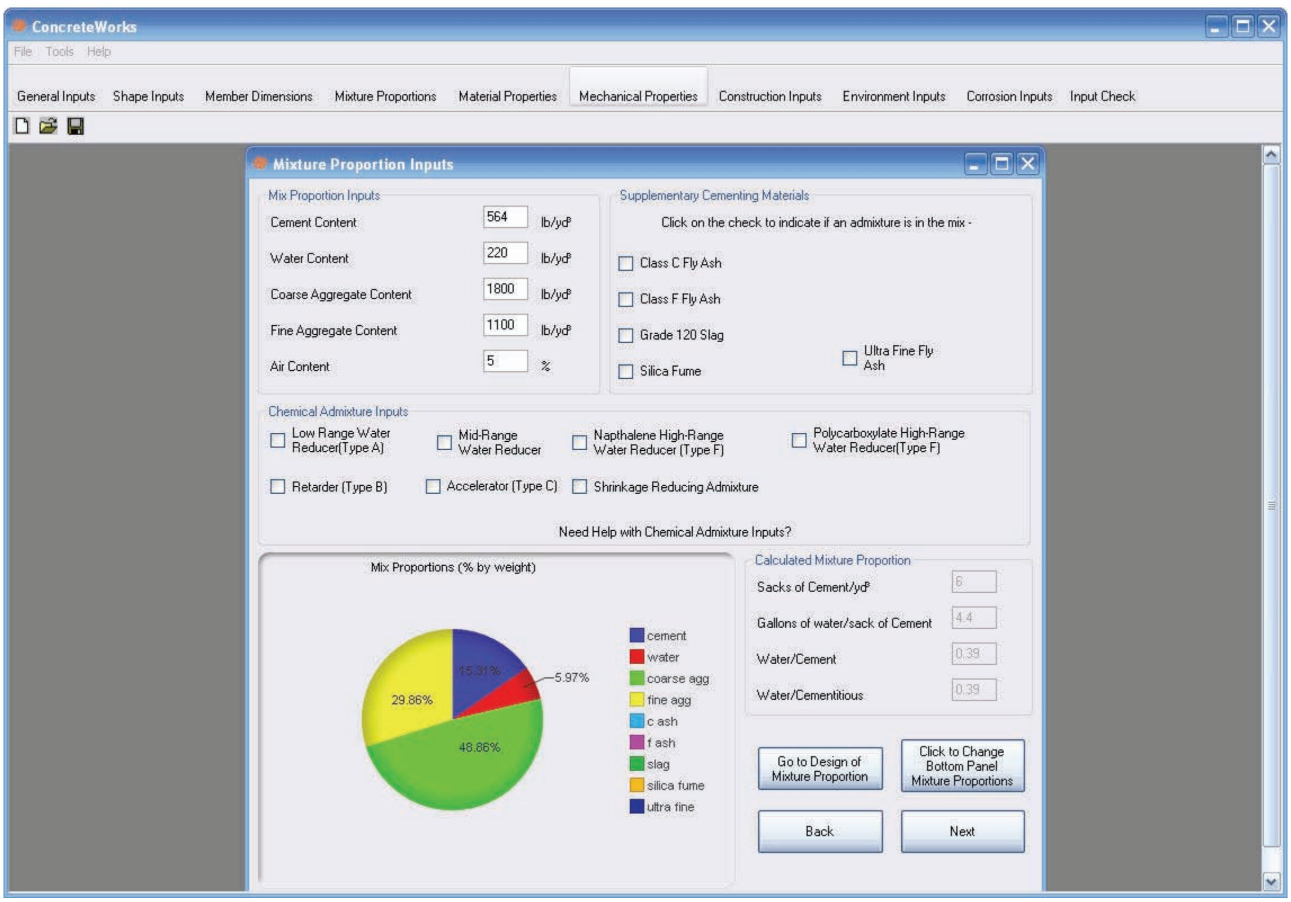

Figure 5.3 "Mixture Proportion Inputs" Screen (Riding 2007)

5.4.2 "Concrete Mixture Proportioning"

The "Design of Mixture Proportion" module is available if the user needs help with the concrete mixture design and proportioning. "Concrete Mixture Proportioning" implements the mixture proportioning steps as found in ACI 211 (1991) and NHI Course 15123 (Hover 2003). For a detailed presentation of the mixture proportioning procedure and limitations, please refer to ACI 211 (1991) and the ConcreteWorks User Manual (Riding 2007). The most important thing to remember about the mixture proportion calculations is that they are only designed to create the proportions for making and testing a trial batch. The calculations in the "Concrete Mixture Proportioning" are not intended to be used as a substitute for local knowledge of material properties or for trial batches. The mixture proportioning guide in ConcreteWorks is designed to be a user-friendly tool that may assist the user in determining the trial batch mixture proportions.

The final volume calculations for the concrete mixture are calculated based on the aggregate properties, cement content, adjusted water content, mineral admixture replacement, and air content. When the total calculated paste content exceeds 30% by volume, a warning appears to the user that the concrete mixture may be more susceptible to drying shrinkage. This warning does not preclude using the concrete mixture, but caution should be used for implementing this mixture in members with a high surface area-to-volume ratio that are exposed to a low relative humidity.

5.5 Material/Mechanical Properties

The material characteristics are also entered by the user. The default cement chemistry and hydration parameters are calculated according to either the Bogue method or the Rietveld method of quantifying the cement composition. The user decides which method is used. The user can also manually override the default cement chemistry and hydration parameters, which are calculated using the equations from Chapter 2 of this report. For example, if the user has performed a semi-adiabatic calorimetry test on the concrete mixture used, then the calculated hydration properties can be changed in order to achieve more accurate results. Most of the testing that was performed in the development of these equations was done using materials from Texas. In the case that the concrete material properties deviate substantially from those used in Texas, a semi-adiabatic calorimetry test should be performed to determine the hydration parameters.

The user can select the type of coarse and fine aggregates used in the concrete batch. The coefficient of thermal expansion (CTE) and material thermal properties are calculated based on the mixture proportions and the coarse aggregate types. The coefficient of thermal expansion and material thermal properties may be inputted by the user if a hardened concrete coefficient of thermal expansion test, hardened concrete thermal conductivity test, or aggregate specific heat test has been performed. It is highly recommended that the user perform a hardened concrete coefficient of thermal expansion test on the concrete mixture to be used because the thermal stresses calculated are very sensitive to the concrete CTE.

Additionally, the user can input the type of maturity method used, the strength-maturity relationships, and the early-age creep parameters. For example, the "Maturity Functions" frame allows the user to select between the Nurse-Saul method of maturity and the equivalent age method, both as described in ASTM C 1074. The concrete early-age creep is calculated using the Modified Linear Logarithmic Model (MMLM) described in the Concrete Works User Manual (Riding 2007). Different equations are used depending on whether the Bogue method or the Rietveld method is selected.

5.6 Construction Inputs

Each type of concrete member will have different construction options to choose from; Figure 5.3 shows a rectangular column as an example. ConcreteWorks automatically displays the needed inputs based on the other options selected by the user (such as member type or if the member is submerged). If the member shape or submerged status is altered, the available construction inputs change. Dramatically different results will be calculated for even small changes in the construction inputs, such as the form type, or blanket insulation.

The concrete placement temperature can be calculated in three ways, using either: the temperature of each of the materials, the ambient temperature, or a manually-entered value. The user chooses which method is used. Additionally, the user also inputs the concrete age when formwork is removed (at the cross-section being analyzed), starting from the time the concrete was first mixed.

The surroundings of the concrete member affect the temperature development as well. User inputs include the temperature of the surrounding water, air, soil, etc., the types of curing methods applied to the member after the forms are removed, which sides of the member use form liners, and the insulation R-value for the cure blankets. There are additional inputs specific to the type of concrete member. For example, for a bent cap, the type of formwork used for the bottom of the bent cap needs to be defined.

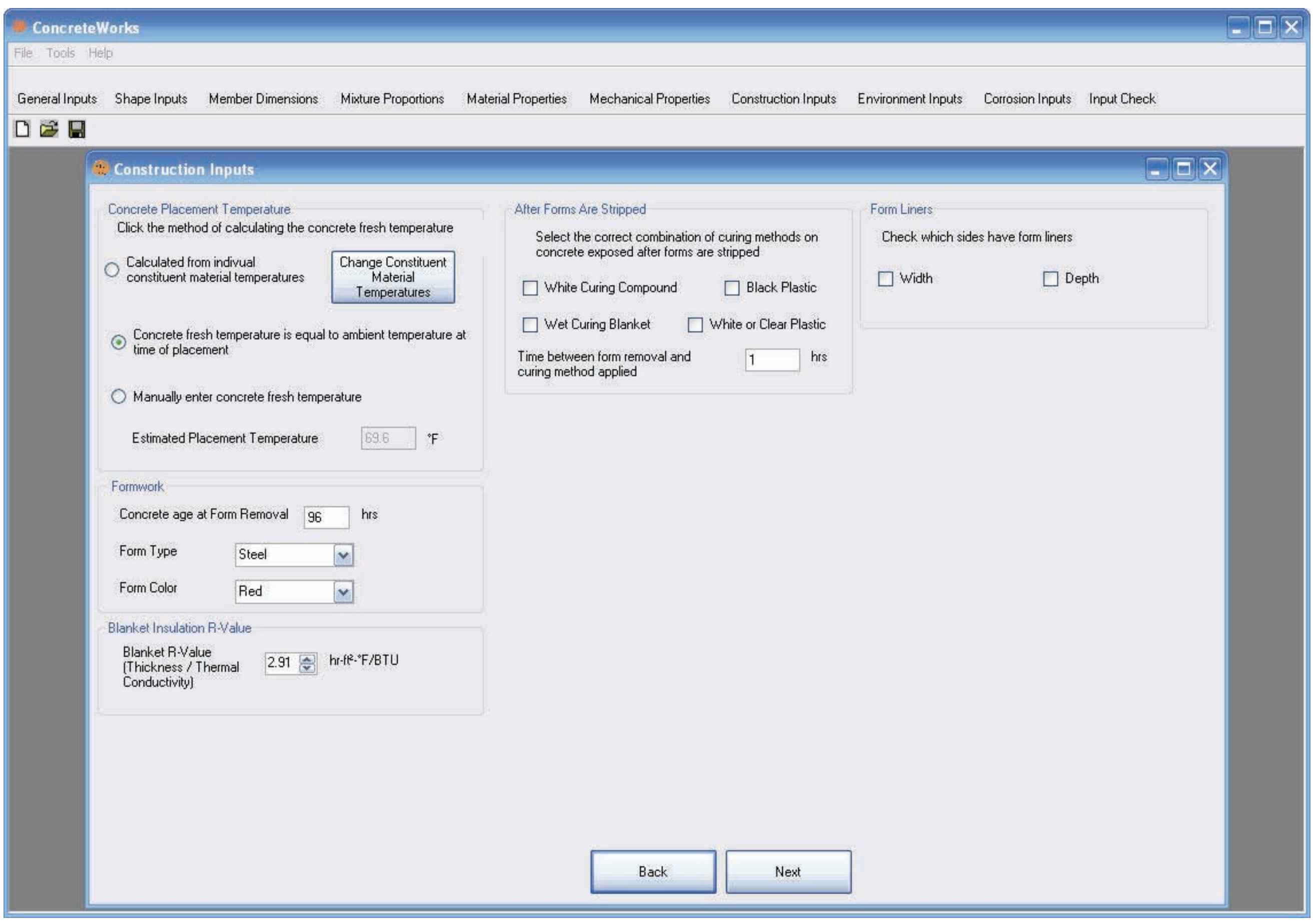

Figure 5.4 "Construction Inputs" Screen for a Rectangular Column (Riding 2007)

5.7 Input Check

An "Input Check" screen shows the values that have been entered. Thus, the user can make sure no mistakes were made in the inputs section of ConcreteWorks. Default values used are highlighted green, and the questionable values are highlighted red. Just because ConcreteWorks deemed the value questionable, does not always mean that the program will not calculate temperature profiles for the element. A red value simply means that the user should check to make sure that the value is indeed what the user wanted to enter. Users should be careful when using these questionable values, because they can sometimes cause instability in the ConcreteWorks program.

5.8 Results

The program is run after the user inputs all the necessary information. The predictions that are obtained from the model are explained below. For a more detailed explanation of the results, see the ConcreteWorks User Manual (Riding 2007). Program features, such as how to save, print, and export files are included in the User Manual as well.

5.8.1 Mixture Checks

A summary table of the calculated results is shown in Figure 5.4. The first section states the set of specifications used to check the calculated results, the maximum temperature in the concrete member during the analysis period, the maximum temperature difference at time *t* anywhere in the concrete member, and whether the concrete mixture meets the specifications selected for alkali silica reactivity. The second section informs the user the time to corrosion initiation and damage expected in the concrete member.

The last section gives the cracking probability classification. A low or moderate cracking probability classification does not guarantee that the structural member will be free of cracks. A low cracking probability classification only indicates that the probability of cracking is lower than if the concrete cracking probability classification were moderate, high, or very high. Any classification, including the low cracking probability classification includes some chance that cracking will occur. When the TxDOT 2004 specification is selected, the maximum temperature difference line in the table will be highlighted red if the value exceeds 35° F (20° C), the maximum temperature in the member line will be highlighted if the value exceeds 158° F (70° C), and the alkali-aggregate reactivity line will be highlighted red if the concrete does not meet TxDOT specification 421 (TxDOT, 2004b).

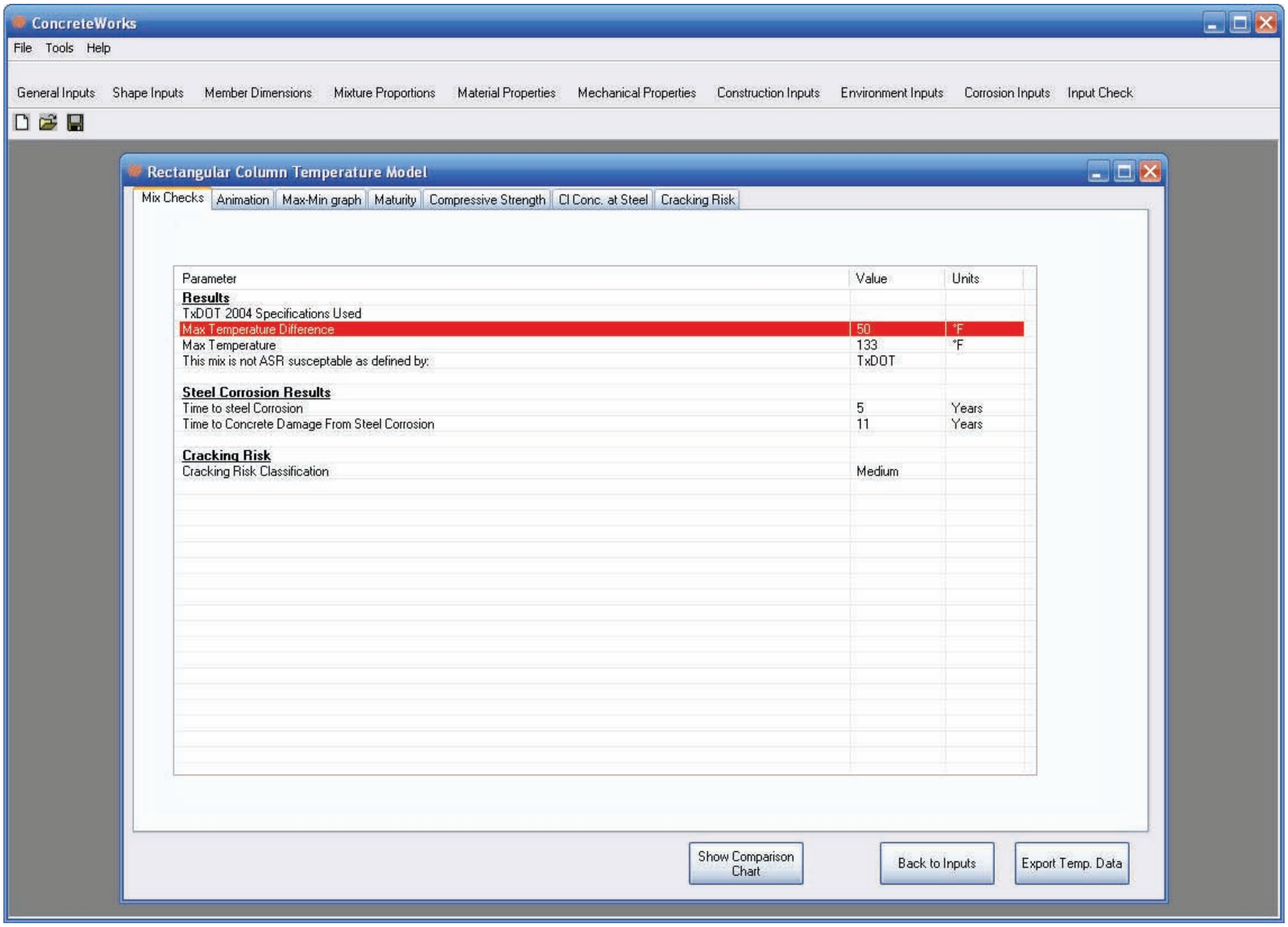

Figure 5.5 "Mix Checks" Tab for a Rectangular Column (Riding 2007)

5.8.2 Graphs

The development of a property versus time calculated by ConcreteWorks can be graphed. The "Max-Min Graph" tab shows the user a graph of the important calculated values with time. The values shown are: the maximum temperature anywhere in the concrete member at each point in time, the minimum temperature anywhere in the concrete member at each point in time, the maximum temperature difference in the concrete member at each point in time, and the ambient temperature.

The user may also access a graph that shows the calculated maximum, minimum, and maximum maturity difference for the concrete member. The maturity is calculated from the strength parameters chosen by the user prior to running the program. The calculated maturity is an estimate and only applies when the maturity parameters entered are from the same concrete mixture used on the project.

The "Compressive Strength" tab shows the maximum compressive strength, minimum concrete strength, and the average compressive strength of the concrete member. The compressive strength is calculated using the predicted concrete temperature, the calculated concrete maturity (as described in the ConcreteWorks User Manual (Riding 2007)), and the compressive strength parameters entered by the user. The concrete compressive strength is only calculated if the user enters the compressive strength parameters among the mechanical properties prior to running the program.

As part of the chloride service life analysis, ConcreteWorks calculates the chloride concentration profile in the concrete member. ConcreteWorks plots the chloride concentration versus time at the steel depth. When the chloride concentration reaches the chloride threshold level, corrosion is considered to have initiated. The chloride concentration value at the steel level will turn orange once corrosion exceeds the chloride threshold level to notify the user of the point in time after mixing at which corrosion initiation is predicted to occur.

The cracking risk classification at different times is plotted as a colored bar chart, with the maximum temperature difference plotted as a blue line on the same graph to show how the temperature gradient in the concrete affects the cracking risk classification. Figure 5.5 shows the graph used to show the cracking risk classification and maximum temperature difference. The bar color shown for the cracking risk classification corresponds to the classification shown at the bottom of the chart. The methodology used to determine the cracking risk classification is discussed in the ConcreteWorks User Manual (Riding 2007). A green color corresponds to a low cracking risk classification, yellow to moderate, orange to high, and red to a very high cracking risk classification.

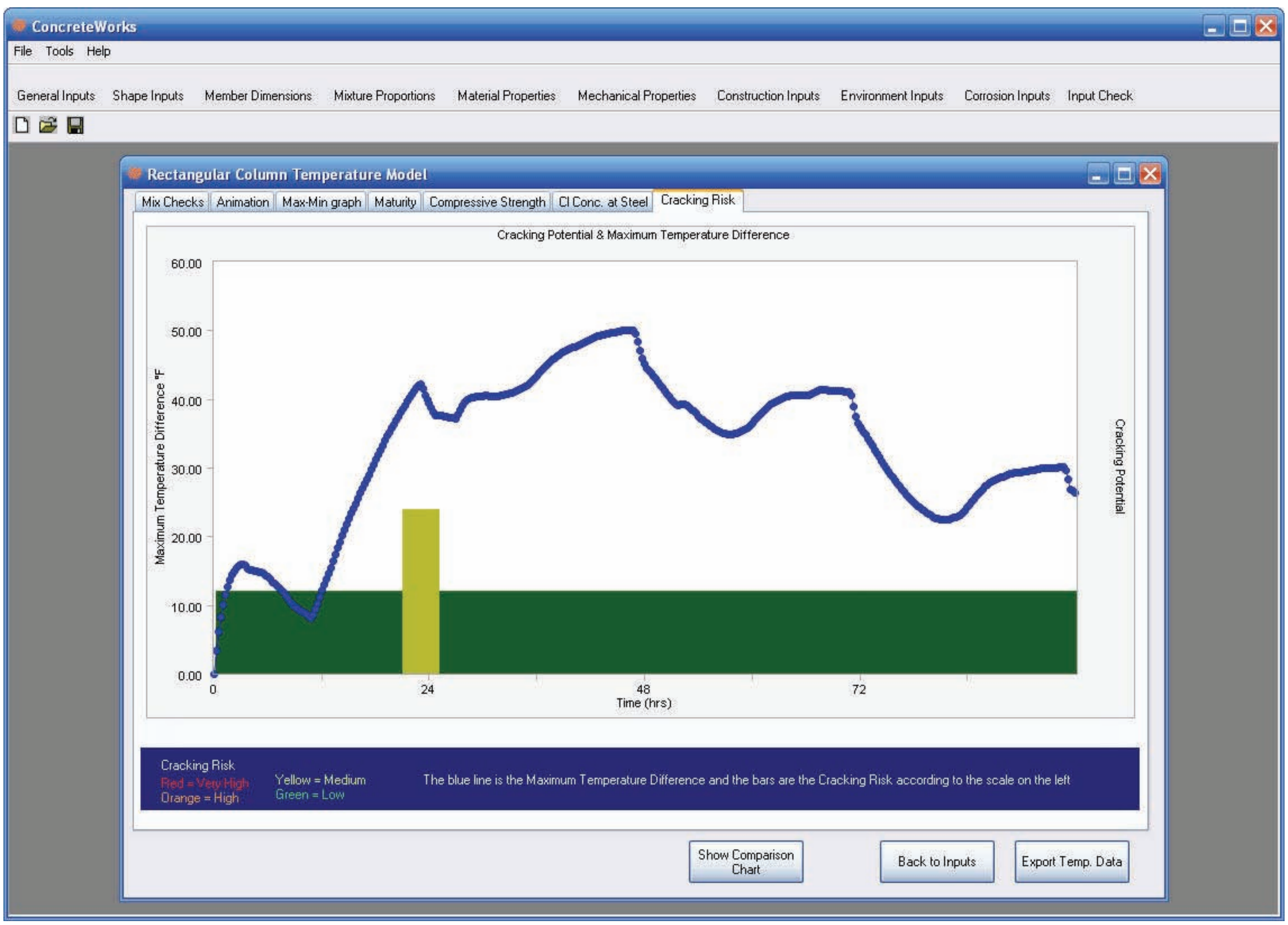

Figure 5.6 Cracking Risk Classification Chart (Riding 2007)

5.8.3 Animation

The user may view an animated chart of the concrete member, displaying a property of concrete varying across the cross-section. For members modeled taking into account three dimensions, either of the cross-sections can be displayed. The graphic will change as the displayed time changes. Compressive strength, maturity, and temperature are among the items that can be animated. Figure 5.6 shows varying temperature across a rectangular column's cross-section. As expected, the temperature near the center of the column is higher than the temperature on the sides due to the heat produced by hydration.

When the cracking failure classification is calculated, the animation will also display a bar at the bottom of the animation that will show the cracking classification at the point in time that is being animated.

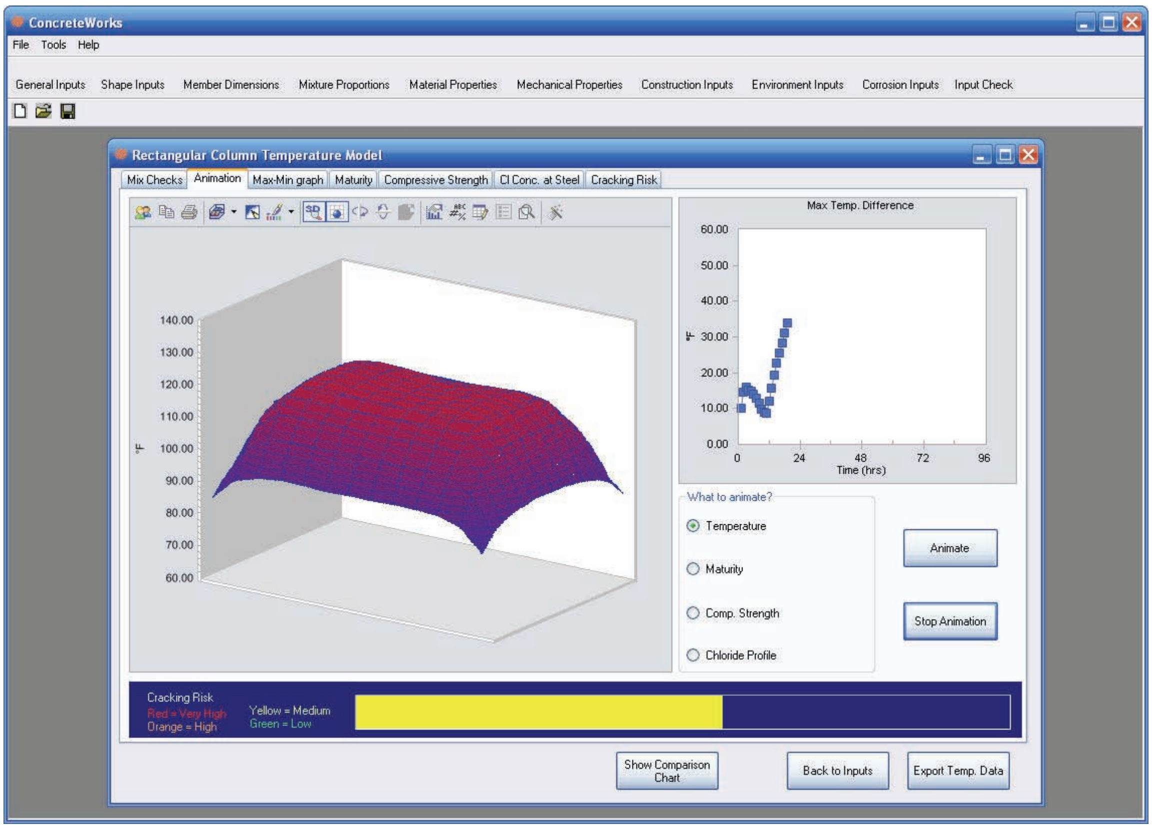

Figure 5.7 "Animation" Tab for a Rectangular Column (Riding 2007)

5.8.4 Show Comparison Chart

The user may compare results from different analysis runs. The "Show Comparison Chart" screen allows the user to compare calculated maximum temperatures, maximum temperature differences, cracking probability classifications, and chloride concentration levels at the steel. Thus, different options for a mixture can be compared and contrasted so that the most cost-effective option can be adopted.

6. Project Implementation

The following chapter describes how results of this research should be implemented for use by TxDOT. In addition to the ConcreteWorks software, a series of video tutorials are available. Results from the research have been published in theses, dissertations, magazines, journals, and conference proceedings. At the end of this chapter, a list of recommended specification changes is presented.

6.1 Technology Transfer

As part of this research project, a methodology for quantifying the early-age concrete heat of hydration and creep compliance has been developed. The tests required, correct testing procedures, and analysis methods have been documented in this report and the accompanying documents. Additionally, a website has been developed to distribute the ConcreteWorks software package free of charge at www.texasconcreteworks.com. To download the software package, users are required to register with the website. The number of registered website users serves as an indication of the interest and applicability of the software to the engineering and construction industry. To date, several hundred engineers and contractors from around the world have registered on the website and downloaded ConcreteWorks.

6.2 Training

A critical part of the research implementation plan is the training of engineers, contractors, and material suppliers on the correct application of ConcreteWorks. A user manual has been written that documents the theory and assumptions used in developing the software. The user manual also contains an operator's manual that explains the software features and how to use the software. Demonstrations of the software have been given at project advisory meetings, conferences, and two training workshops given in December 2005 in Fort Worth, Texas.

To further facilitate training of users on the use of ConcreteWorks, a series of video tutorials has been created. The video tutorials demonstrate the features available and how to correctly change inputs for each input screen in the software. A narrative is provided that explains what each input does and how to use the software features. Two video tutorials are included that walk the user through two example cases of how to correctly use the temperature prediction, cracking probability classification, and chloride service life modules included in Version 2 of ConcreteWorks. The first example describes the iterative design process for a rectangular column to limit the thermal stress cracking probability while decreasing the form cycling time. The second example describes the use of the bridge deck temperature prediction and chloride service life modules. Also, a demonstration shows the user how to use the bridge temperature prediction to determine if the bridge deck temperature during curing will be unacceptably low. The ConcreteWorks version 2 software tutorials are available to download from www.texasconcreteworks.com.

6.3 Trial Software Use

A beta version of ConcreteWorks was delivered to TxDOT for trial use and testing in October 2003. ConcreteWorks Version 1 was delivered to TxDOT for trial use and implementation. The use of ConcreteWorks Version 1 has been specified in several projects by TxDOT in Fort Worth and El Paso. Additionally, ConcreteWorks Version 1 has been used successfully by material suppliers working on a project for the Dallas Area Rapid Transit. During the trial use of ConcreteWorks Version 1, several suggestions for improvement of the software were made to increase the ease of implementation of ConcreteWorks Version 2. The changes made for Version 2 include, but are not limited to, a feature to export the inputs to SiteManager, a PDF report feature, and a tool to compare different analysis iterations. ConcreteWorks Version 2 is expected to provide TxDOT with a valuable tool for increasing the durability of concrete bridge members while at the same time allowing for innovation and lower construction costs. It is strongly recommended that TxDOT perform trial field applications of ConcreteWorks Version 2.

6.4 Public Dissemination of Research

A concerted effort has been made to widely disseminate the research and software developed as part of this project. To date, three technical papers have been published in the *American Concrete Institute Materials Journal*, two technical papers have been published in *Special Publication 241* of the American Concrete Institute, and one magazine article has been published in *Concrete Construction*. It is anticipated that several additional technical papers will be submitted for publication in peer refereed archival journals. Additionally, the ConcreteWorks software package and accompanying user manual and video tutorials are available to the public for download free of charge.

Much more detail on the laboratory evaluations, field studies, and modeling efforts can be found in Ph.D. dissertations by Poole (2007) and Riding (2007), as well as MS theses by Whigham (2005) and Meadows (2007).

6.5 Specification Changes

Currently, TxDOT specification 420.4 restricts the placement temperature of mass concrete to between 50 (10 °C) and 75° F (23.9 °C). The specification also limits the maximum concrete core temperature to 160° F (71.1 °C) and the maximum temperature differential between the concrete core and the concrete surface to 35° F (20 °C). These specifications have greatly reduced the incidence of thermal cracking in mass concrete structures in Texas. These specifications may be overly conservative for some situations. Considerable cost savings may result from changes in the specifications that allow for innovation while still maintaining an adequate level of protection against thermal cracking.

The maximum in-place temperature limit specification was developed to prevent delayed ettringite formation from occurring in mass concrete members. The current maximum temperature limit of 158° F (70 °C) could be changed to that in Table 6.1 to be more consistent with current temperature limits for precast concrete.

Table 6.1 Proposed Maximum in-Place Temperature Limit Specification

Maximum In-Place Concrete Temperature (*T_{max}*)	Prevention Required
T_{max} < 158°F (70 °C)	None.
158°F (70 °C) ≤ T_{max} ≤ 185°F (85 °C)	Use one of the following approaches to minimize the risk of DEF: 1. Use portland cement that meets the requirements of ASTM C 150 for Type II, IV, or V cement and has a Blaine fineness ≤ .58 psi (400 m^2/kg) 2. Use portland cement with a 1-day mortar strength (ASTM C 109) ≤ 20 MPa 3. Use any of the following suitable combinations of pozzolan or GGBF slag with portland cement: —at least 25% fly ash meeting the requirements of ASTM C 618 for Class F fly ash —at least 35% fly ash meeting the requirements of ASTM C 618 for Class C fly ash —at least 35% GGBF slag meeting the requirements of ASTM C 989 —5% silica fume (meeting ASTM C 1240) in combination with at least 25% GGBF slag.
T_{max} > 185°F	This condition is not allowed.

The maximum temperature differential specification could also be changed. Stress analyses are an important tool in developing mass concrete temperature control plans, designing concrete mixture proportions, and determining construction practices. It is very difficult, however, to measure the concrete in-place stress development to verify compliance with the temperature control plan. Any specification developed should require the contractor to instrument the mass concrete member for temperature development to ensure that the temperature differential does not become excessive. The allowable maximum temperature differential to reduce the probability of thermal cracking should be different, however, for different type and size concrete members and materials used. As the concrete tensile strength increases, the concrete's ability to withstand temperature changes increases.

During the mixture submittal phase of all mass concrete projects, ConcreteWorks should be used to determine the concrete mixture and construction practices for the specific site conditions to obtain a low to moderate cracking risk. Once the mixture is approved for use, measurement of the in-place concrete temperatures and temperature differences are still required to ensure that appropriate contracting procedures are followed.

The maximum temperature difference should be measured using one temperature sensor placed in the center and one at the cover between 1.5 and 2.5 inches from the concrete surface. For rectangular columns, the surface probe should be located in the middle of the side with the longest dimensions, as shown in Figure 6.1. In the case that insulation or an architectural form liner is used on only the sides of the column with the longest dimensions, an additional edge probe should be used on adjacent sides, as shown in Figure 6.2. In this case, the temperature difference recorded from the center probe to either edge probe should stay below the prescribed maximum temperature differential limits.

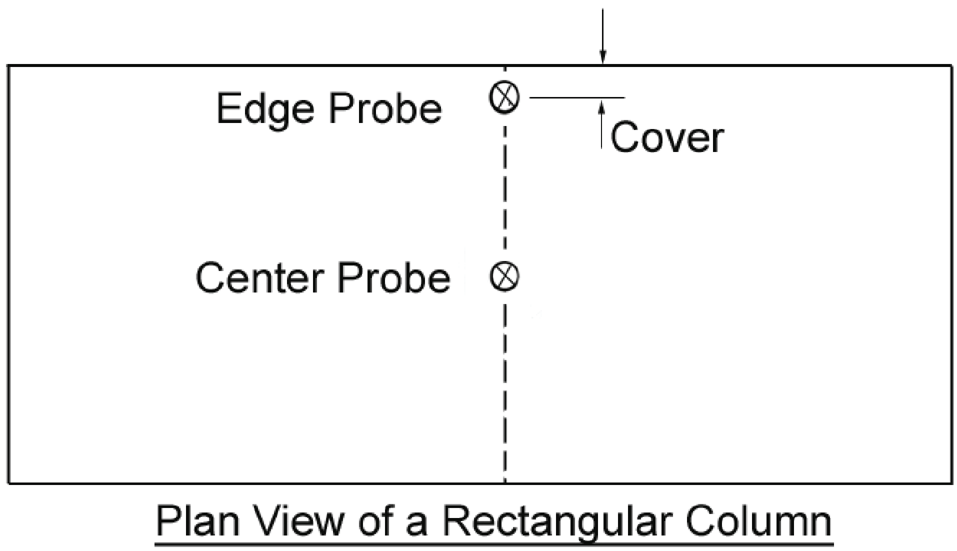

Figure 6.1 Temperature sensor locations for a rectangular column

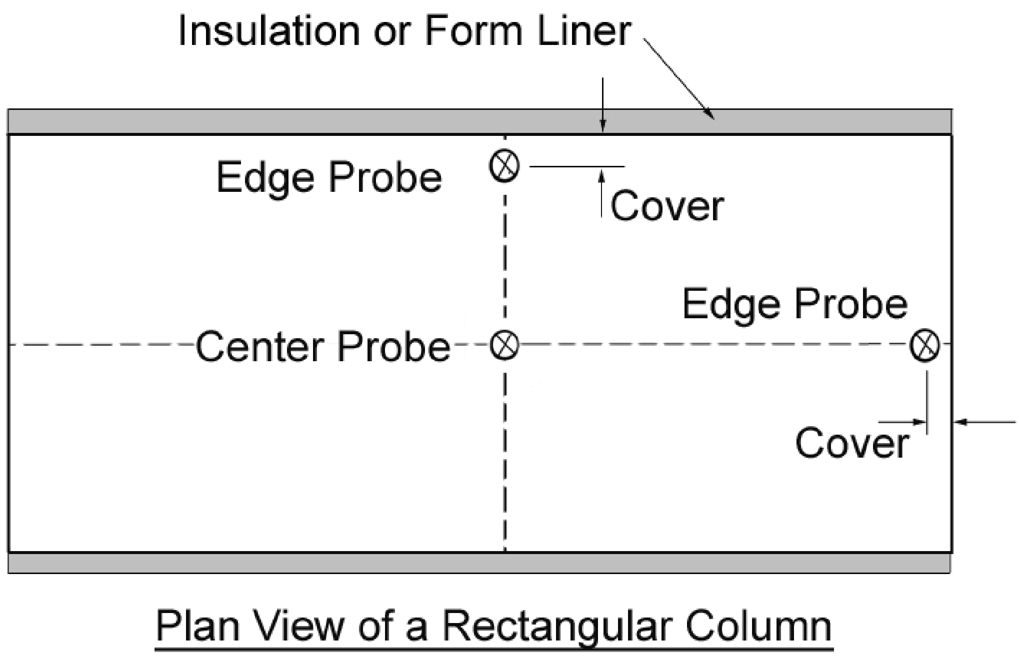

Figure 6.2 Temperature sensor placement for a rectangular column with insulation or a form liner on the longer of the two plan dimensions

The specification that limits the maximum temperature differential allowable during construction could be altered to allow higher maximum temperature differentials when more tests are performed to better characterize the concrete mixture used. The three proposed options are:

1. Keep the specification unchanged; therefore, the maximum temperature difference for all mass concrete members is limited to 35° F (20° C).
2. Use a temperature difference modification factor (TDMF); the maximum temperature difference is determined by the compressive strength development, concrete member size, and concrete coefficient of thermal expansion as per TxDOT test method Tes-428A. An example of a TDMF chart for a rectangular column is shown in Figure 6.3. The TDMF chart for other concrete member types will need to be developed as part of future research. The least column dimension shown in Figure 6.3 is the least dimension of a rectangle that contains the whole rectangular column. The maximum temperature difference selected for the temperature difference modification factor varies with the in-place concrete compressive strength, as shown in Figure 6.4. The in-place concrete compressive strength is determined using a concrete strength-maturity relationship previously developed during the mixture prequalification and the temperature history measured at the concrete surface. The maximum temperature difference is limited to between 20° F (-6.67° C) and 60° F (15.6° C).
3. Specify a maximum temperature difference developed from a concrete thermal stress analysis.

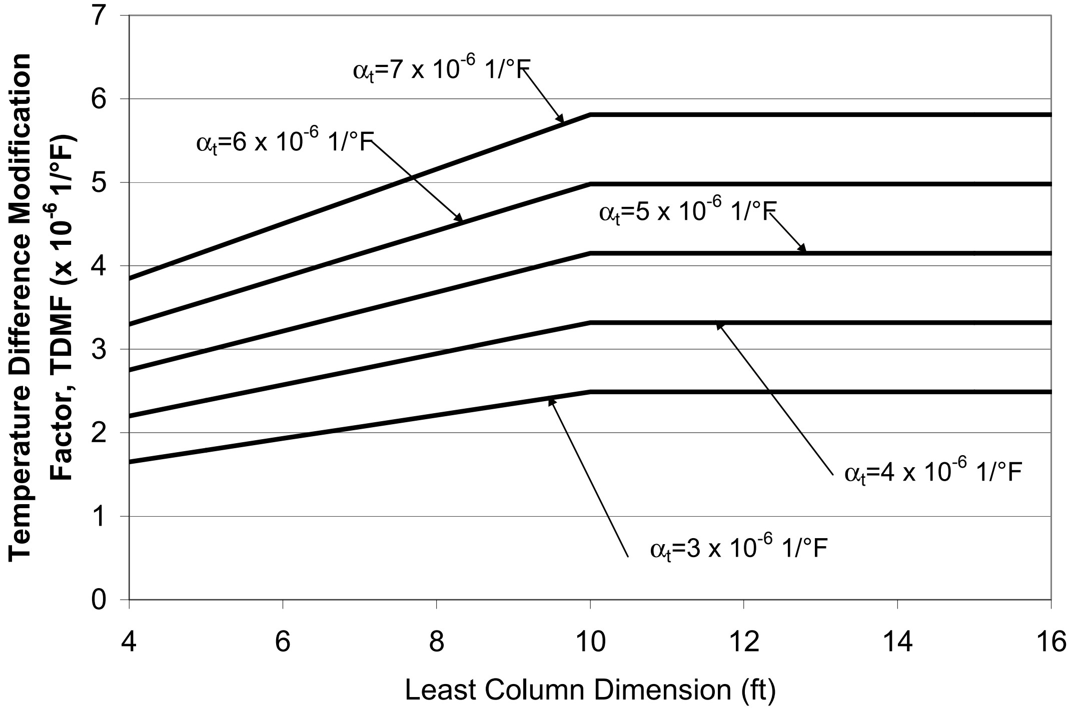

Figure 6.3 Temperature Difference Modification Factor Chart for a Rectangular Column

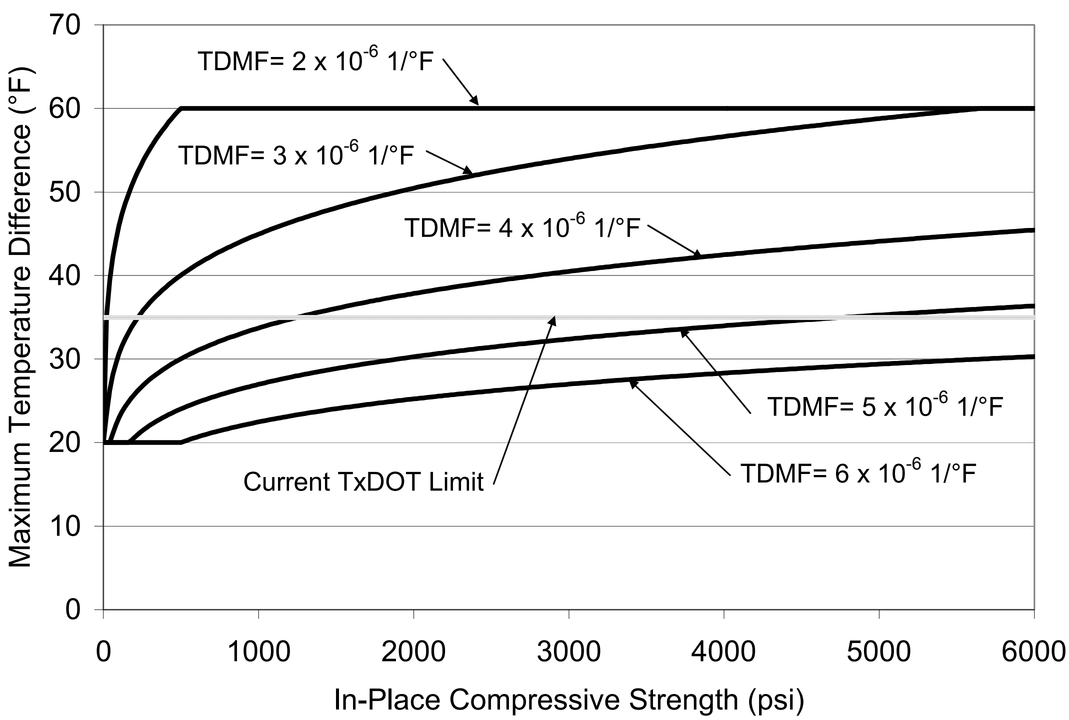

Figure 6.4 Maximum temperature Difference Versus the in-place Concrete Compressive Strength for Different Temperature Difference Modification Factors

6.6 User Feedback

It is recommended that TxDOT evaluate the usefulness of ConcreteWorks by surveying ConcreteWorks users that are actively involved with the design and construction process. The feedback obtained from such a survey could be used as a roadmap for future software improvements, and could be considered when gauging the success of the project.

7. Conclusions

7.1 Summary

ConcreteWorks provides engineers, contractors, and inspectors with a user-friendly tool for quantifying concrete material behavior, particularly the heat generation and cracking risk of mass concrete members in transportation structures. In order to develop the software, significant research was performed to quantify early-age concrete behavior. A heat of hydration model was developed in which a non-linear regression analysis was used to produce equations for the activation energy of cementitious systems, as well as models to quantify the heat of hydration development. Different models were developed for cement compositions determined by the Rietveld and Bogue methods. These models account for mixture proportions, cement and SCM chemistry, and chemical admixture dosages.

To complete the temperature prediction model, the effects of geometry, formwork type, and environmental conditions needed to be quantified as well. An analysis of the heat conduction in the concrete, the heat generation from the hydration process, and the heat exchanged at the boundary of the structural element was carried out. Once the model was completed, the results were compared with field site data to validate its effectiveness.

Next, early-age concrete property development was modeled using results from rigid cracking frame results and splitting tensile, elastic modulus, and compression testing. A non-linear multivariate model for predicting creep was developed based on concrete constituent material properties and mixture proportions from Rietveld or Bogue data. Failure criteria to calculate the probability of concrete cracking based on the concrete tensile strength-to-splitting tensile strength ratio were also developed.

ConcreteWorks allows the user to input the member dimensions, environmental conditions, and formwork properties, as well as time and location. The program predicts the temperature development in the member and assesses the cracking potential.

7.2 Economic Benefits

A thorough analysis on the economic benefits of using ConcreteWorks has not been carried out. However, significant savings can be expected at several different stages of projects for which ConcreteWorks is used. In the design stage, the engineer can run ConcreteWorks with mixes containing different kinds of local aggregates in order to create an efficient mix design while minimizing cost.

In the construction stage, contractors can use ConcreteWorks instead of more complex and expensive analysis to develop a thermal stress control plan. Furthermore, ConcreteWorks can be used to assess when formwork may be removed. Removing formwork earlier will result in speedier construction and thus reduced overall costs.

Most importantly, the savings in avoiding repairing or replacing bridges will be significant. Repairing or replacing bridges that are *not* functionally obsolete is very costly. The most critical time for assuring a long service life for a concrete structure is before and during construction. Proper use of ConcreteWorks during the design and construction stages will result in these unexpected problems being avoided. Also, with the chloride ingress model structures can be designed for greater durability, so that future maintenance and replacement costs can be reduced.

7.3 Additional Research

The following additional research is recommended:

1. A more accurate autogenous shrinkage model would be useful, as the model currently used in ConcreteWorks can be improved. Presently, there are no models available that can accurately model any early-age concrete autogenous expansion. Also, the effects of supplementary cementing materials and temperature on are not included.
2. Thermal stress development on bridge decks could be studied using rigid cracking frames. The relative stress development, including any beneficial thermal pre-compression for different concrete materials and construction techniques could be examined using the procedure outlined in this study.
3. A field calibration and validation of the ConcreteWorks bridge deck temperature development module when precast panels or wood formwork are used would add to the accuracy of the software. A field validation of the effects of cold weather on bridge deck temperature development should be studied as well.
4. Thermal stress development on pavements could be studied as well, also taking into account drying shrinkage. Special attention could also be given to long-term drying shrinkage when lightweight aggregate is used.
5. More cracking frame tests should be carried out in order to improve the existing model. Very little testing was done with high volumes of fly ash or slag since the focus was on the most commonly used replacement materials and amounts.
6. T-shaped bent caps and circular columns could be included in the stress prediction model.
7. Chloride profile grinding should be carried out to determine the chloride surface concentration on bridge decks in the field. These data could be used to calibrate the existing model.
8. The effects of lightweight aggregates on temperature development are not well known. These effects should be quantified with research and calibrated with field site data.
9. A procedure for using simple calorimetric devices as a screening test for bad mixtures should be developed.

References

ACI Committee 211, "Standard Practice for Selecting Proportions for Normal, Heavyweight, and Mass Concrete, ACI 211.1R, American Concrete Institute, Farmington Hills, Mich., 1991, pp. 38.

ACI Building Code Committee, 2005, "Building Code Requirements for Structural Concrete (ACI 318-05) and Commentary (ACI 318R-05)," American Concrete Institute, Farmington Hills, MI, pp 430.

ACI Committee 207, "Effect of restraint, volume change, and reinforcement on cracking in massive concrete," ACI 207.2R, American Concrete Institute, Farmington Hills, Mich., 1995, pp. 3-10.

ACI Committee 207, "Guide to Mass Concrete," ACI 207.1R-05, American Concrete Institute, Farmington Hills, Michigan, 2005.

Altoubat, S.A., 2000, "Early Age Stresses and Creep-Shrinkage Interaction of Restrained Concrete," Doctoral Thesis, the University of Illinois at Urbana-Champaign, pp. 221.

ASTM C 105, 2005, "Standard Specification for Portland Cement," ASTM International, West Conshoocken, PA., pp. 8.

ASTM C 204, 2005, "Standard Test Method for Fineness of Hydraulic Cement by Air Permeability Apparatus," ASTM International, West Conshoocken, PA., pp. 10.

ASTM C 403, 2006, "Standard Method for Time of Setting of Concrete Mixtures by Penetration Resistance," ASTM International, West Conshoocken, PA., pp. 7.

ASTM C 1074, 2004, "Standard Practice for Estimating Concrete Strength by the Maturity Method," ASTM International, West Conshoocken, PA, pp. 9.

Chini, A.R., Muszynski, L. C., Acquaye, L., and Tarkhan, S., "Determination of the Maximum Placement and Curing Temperatures in Mass Concrete to Avoid Durability Problems and DEF," Final Report, University of Florida, July 2003, pp. 46-64.

Emborg, M., "Models and Methods for Computation of Thermal Stresses," Prevention of Thermal Cracking in Concrete at Early Ages, Edited by R. Springenschmid, RILEM Report 15, EF Spon, London, 1998, pp 178-230.

Folliard, K.J., Barborak, R., Drimalas, T., Du, L., Garber, S., Ideker, J., Ley, T., Williams, S., Juenger, M., Fournier, B. and M.D.A. Thomas, Preventing ASR/DEF in New Concrete: Final Report, Research Report No.0-4085-5, Center for Transportation Research, The University of Texas at Austin, 2006. pp. 2-3.

Freiesleben Hansen, P., and E.J. Pedersen, "Curing of Concrete Structures," CEB Information Bulletin 166, 1985, pp. 24.

Freiesleben Hansen, P., and E.J. Pedersen, “Maturity computer for controlling curing and hardening of concrete,” *Nordisk Betong*, V. 1, No. 19, 1977, pp. 21-25.

Grasley, Z.C., 2006, “Measuring and Modeling the Time-Dependent Response of Cementitious Materials to Internal Stresses,” Doctoral Thesis, The University of Illinois at Urbana Champaign, pp. 238.

Hover, K., “NHI Course 15123 – Highway Materials Engineering: Portland Cement Concrete Module – Participant Workbook,” 2003.

Incropera, F.P.; and Dewitt, D.P., Fundamentals of Heat and Mass Transfer, John Wiley & Sons, Inc., New York, 2002, p. 931.

Mangold, M. Methods for Experimental Determination of Thermal Stresses and Crack Sensitivity in the Laboratory. In *Rilem Report 15, Prevention of Thermal Cracking in Concrete at Early Ages*, Edited by R. Springenschmid, E & Fn Spon, London, 1998, pp. 26-39.

Mindess, S., Young, J.F., and Darwin, D., Concrete, 2nd Ed., Pearson Education, Inc., Upper Saddle River, NJ, 2003.

Patankar, S.V., Numerical Heat Transfer and Fluid Flow, McGraw-Hill Book Company, New York, 1980, p. 30-66.

Poole, J.L., “Methods of Activation Energy Calculation for Portland Cement,” Master’s Thesis, The University of Texas at Austin, 2004, pp. 75.

Poole, J.L., “Modeling Temperature Sensitivity and Heat Evolution of Concrete,” PhD Dissertation, The University of Texas at Austin, Austin, TX, 2007.

Riding, K.A., Poole, J.L., Schindler, A.K., Juenger, M.C.G., Folliard, K.J., “Temperature Boundary Condition Models for Concrete Bridge Members,” ACI Materials Journal, 2007.

Riding, Kyle, “Early Age Concrete Thermal Stress Measurement and Modeling,” PhD Dissertation, The University of Texas at Austin, Austin, TX, 2007.

Schindler, A.K., “Concrete Hydration, Temperature Development, and Setting at Early-Ages,” Doctoral Dissertation, The University of Texas at Austin, 2002, 530 pp.

Schindler, A.K., and K.J. Folliard, “Heat of Hydration Models for Cementitious Materials,” *ACI Materials Journal*, V. 102, No. 1, Jan.-Feb., 2005, pp. 24-33.

Scrivener, K.L., T. Füllmann, E. Gallucci, G. Walenta, and E. Bermejo, “Quantitative Study of Portland Cement Hydration by X-Ray Diffraction/Rietveld Analysis and Independent Methods”, *Cement and Concrete Research*, V. 34, 2004, pp 1541-1547.

Springenschmid, R. and R. Breitenbücher. Influence of Constituents, Mix Proportions and Temperature on Cracking Sensitivity of Concrete. In *Rilem Report 15, Prevention of Thermal*

Cracking in Concrete at Early Ages, Edited by R. Springenschmid, E & Fn Spon, London, 1998, pp. 40-50.

TxDOT, 2004a, “Special Provision 420 – Concrete Structures,” Texas Department of Transportation.

TxDOT, 2004b, “Special Provision 421 – Hydraulic Cement Concrete,” Texas Department of Transportation.

Tex-428-A, 2001, “Determining the Coefficient of Thermal Expansion for Concrete,” Texas Department of Transportation, Standard Test Procedures, pp. 8.

Thomas, J.J., and Jennings, H.M., 2006, “A Colloidal Interpretation of Chemical Aging of the C-S-H Gel and its Effects on the Properties of Cement Paste,” Cement and Concrete Research, Vol. 36, No. 1, pp. 30-38.

Turcry, Philippe, Loukili, Ahmed, Laurent, Barcelo, Casabonne, Jean Michel, “Can the maturity concept be used to separate the autogenous shrinkage and thermal deformation of a cement paste at early age?,” Cement and Concrete Research, 2002.

Van Breugel, K., “Prediction of Temperature Development in Hardening Concrete”, *Prevention of Thermal Cracking in Concrete at Early Ages*, RILEM Report 15, E & FN Spon, London 1998.

Viviani, M., “Monitoring and Modeling of Construction Materials During Hardening,” Doctoral Thesis, Swiss Federal Institute of Technology, Lausanne, Switzerland, 2005, pp. 172.

Westman, G., 1999, “Concrete Creep and Thermal Stresses,” *Doctoral Thesis*, Luleå University of Technology, Division of Structural Engineering, 301 pp.

Whigham, J., “Evaluation of Restraint Stresses and Cracking in Early-Age Concrete with the Rigid Cracking Frame,” Master’s Thesis, Auburn University, 2005.

Young, Francis J., Mindess, S., Gray, R.J.,Bentur, A., The Science and Technology of Civil Engineering Materials, Prentice Hall, Inc., New Jersey, 1998, pp. 241-245.